(1)

J001

AD A116473

RF ABSORPTION BY SUBMICRON METALLIC PARTICLES

William A. Janos
8381 Snowbird Drive
Huntington Peach, California 92646

31 August 1981

Final Report
1 September 1980 - 31 August 1981

Approved for public release; distribution unlimited

Prepared for

OFFICE OF NAVAL RESEARCH
800 North Quincy Street
Arlington, Va. 22217

<<ENTER NEXT COMMAND>>

OF 1

- TITLE: (U) RF ABSORPTION BY SUBMICRON METALLIC PARTICLES
- AGENCY ACCESSION NO: DN075682
- PRIMARY PROGRAM ELEMENT: 61153N
- PRIMARY PROJECT NUMBER: RR02101
- PRIMARY PROJECT AGENCY AND PROGRAM: RR02101
- PRIMARY TASK AREA: RR0210101
- WORK UNIT NUMBER: NR371-027
- CONTRACT/GRANT NUMBER: N00014-80-C-0926
- DOD ORGANIZATION: OFFICE OF NAVAL RESEARCH (427)
- DOD ORG. ADDRESS: DEPARTMENT OF THE NAVY ARLINGTON, VIRGINIA 22217
- RESPONSIBLE INDIVIDUAL: DIMMOCK, J. O.
- RESPONSIBLE INDIVIDUAL PHONE: 202-696-4216
- DOD ORGANIZATION LOCATION CODE: 5110
- DOD ORGANIZATION SORT CODE: 35832
- DOD ORGANIZATION CODE: 265250
- PERFORMING ORGANIZATION: WILLIAM A. JANOS
- PERFORMING ORG. ADDRESS: 8381 SNOWBIRD DR. HUNTINGTON BEACH, CALIFORNIA 92646
- PRINCIPAL INVESTIGATOR: JANOS, W. A.
- PRINCIPAL INVESTIGATOR PHONE: 714-538-7848
- PERFORMING ORGANIZATION LOCATION CODE: 06
- PERF. ORGANIZATION TYPE CODE: 4
- PERFORMING ORG. SORT CODE: 25069
- PERFORMING ORGANIZATION CODE: 395553
- TECHNICAL OBJECTIVE: (U) THE OBJECTIVE IS TO INVESTIGATE THE ELECTROMAGNETIC ABSORPTION AND SCATTERING PROPERTIES OF METALLIC PARTICLES SMALLER THAN AN ELECTRIC SKIN DEPTH, WHICH MAY HAVE APPLICATIONS IN NAVAL COUNTERMEASURES.
- KEYWORDS: (U) ELECTROMAGNETIC SCATTER ,(U) THOMSON SCATTER ,(U) ELECTROMAGNETIC ABSORPTION ,(U) SUBMICRON PARTICLES ,
- DESCRIPTORS: (U) ABSORPTION ,(U) ELECTROMAGNETIC SCATTERING ,(U) ELECTROMAGNETIC RADIATION ,(U) SCATTERING ,(U) PARTICLES ,(U) PARTICLE SIZE ,(U) METALS,
- DATE OF SUMMARY: 24 OCT 80

***

<<ENTER NEXT COMMAND>>

Unclassified
SECURITY CLASSIFICATION OF THIS PAGE (When Data Entered)

REPORT DOCUMENTATION PAGE	READ INSTRUCTIONS BEFORE COMPLETING FORM
1. REPORT NUMBER: J001	2. GOVT ACCESSION NO.	3. RECIPIENT'S CATALOG NUMBER:
4. TITLE (and Subtitle): RF ABSORPTION BY SUBMICRON METALLIC PARTICLES	5. TYPE OF REPORT & PERIOD COVERED: Final Report 1 September 1980-31 Aug 1981
	6. PERFORMING ORG. REPORT NUMBER:
7. AUTHOR(s): William A. Janos	8. CONTRACT OR GRANT NUMBER(s): N00014-80-C-0926
9. PERFORMING ORGANIZATION NAME AND ADDRESS: William A. Janos, Ph.D 8381 Snowbird Drive Huntington Beach, CA. 92646	10. PROGRAM ELEMENT, PROJECT, TASK AREA & WORK UNIT NUMBERS: 61153, RR021-01-01, NR371-027
11. CONTROLLING OFFICE NAME AND ADDRESS: Office of Naval Research 800 North Quincy Street Arlington, VA., 22217	12. REPORT DATE: 31 August, 1981 13. NUMBER OF PAGES: 122
14. MONITORING AGENCY NAME & ADDRESS(if different from Controlling Office)	15. SECURITY CLASS. (of this report): Unclassified 15a. DECLASSIFICATION/DOWNGRADING SCHEDULE

16. DISTRIBUTION STATEMENT (of this Report)

Approved for public release; distribution unlimited.

17. DISTRIBUTION STATEMENT (of the abstract entered in Block 20, if different from Report)

18. SUPPLEMENTARY NOTES

19. KEY WORDS (Continue on reverse side if necessary and identify by block number)

RF Absorbing
Rayleigh
submicron
metallic particles
skin-depth
depolarizing factor
spheroids
filaments
disks
metal coated spheroidal shells
ultrafine con-conductors
conductivity
permittivity

(over)

20. ABSTRACT (Continue on reverse side if necessary and identify by block number)

A comprehensive treatment is presented of the individual and collective RF absorbing properties of small, dilutely distributed metallic particles, under the conditions that the particles be Rayleigh scatterers having at least one submicron dimension. The particles are assumed spheroidal in shape of solid metal, and metal-layered with a non conducting, RF transparent core.

(Con't)

DD FORM 1 JAN 73 1473 EDITION OF 1 NOV 65 IS OBSOLETE
S/N 0102-LF-014-6601

Unclassified
SECURITY CLASSIFICATION OF THIS PAGE (When Data Entered)

The internal electric field and hence the electric moment of an RF irradiated particle is derived from the perturbation solution to the Green's theorem integral equation depicting the depolarizing effect of the induced surface charge and the power dissipation due to the volume current. The resultant internal field is thus the depolarized incident field within a skin-depth attenuation distance from the particle surface. The depolarizing factor derives naturally from the integral formulation, as the internal solid angle subtended by the surface normal component of the incident electric field.

The efficiency of absorbers is then characterized by their depolarizing factors, conductivities, and A.C. permeabilities for ferromagnetic materials.

Through the conventional Lorentz-Lorenz formulation of the composite permittivity of dilute distributions of particle dipole classes, the power reflection/absorption coefficients of the synthetic dielectric medium are established. The penetration lengths, mass requirements and mean constituent particle dimensions and conductivities are described or prescribed in parametric form for high absorption, and its complement, high reflection within broad frequency bands.

A review is presented of the state of dielectric loading, particle preparation, storage and dispersal. Dispersal kinetics are described for near-vacuum and ambient atmospheric conditions. A brief outline of experimental testing requirements and costs is included.

19.(continued)

permeability	resonant	Stratton-Chu
dielectric	efficient	Scatterer
radar	Mie	aerosol
broadband	Lorentz-Lorenz	loading
ferromagnetic	Clausius Mosotti	
loading	power reflection	

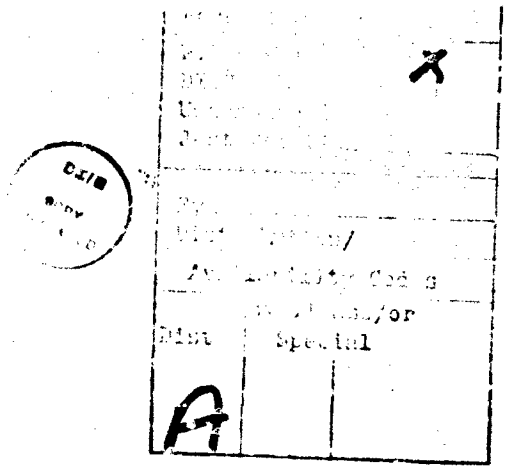

TABLE OF CONTENTS

TABLE OF CONTENTS

TABLE OF CONTENTS

TABLE OF CONTENTS

INTRODUCTION

The component of the incident monochromatic electric vector, $\underline{E}_{o\omega}$, that is normal to the surface of a high conductivity particle induces a surface charge density which essentially neutralizes the net normal component of the field in the interior. For small ratios of particle radius a to free space (or background medium) wave length λ, i.e. $2\pi a/\lambda << 1$, the Rayleigh-Mie solution to the scattered field applies. This is the quasi-electrostatic dipole component induced on a conductor in the presence of a constant longitudinal electric field.[1]

However the tangential component of the incident $\underline{E}_{o\omega}$ vector must also be considered. If the particle size is larger than the skin depth, the net tangential field will have attenuated to zero since enough reradiation will have been generated to cancel the incident tangential field component - the ideal conductor boundary condition that the tangential field is zero.

If the particle size is much less than skin depth, in submicron range for RF - optical frequencies, the tangential field may penetrate into and through portions of the particle, thus driving the interior conduction electrons and generating a volume-distributed, time-variable current density source of additional scattered radiation. For Rayleigh size particles with small relative surface area normal to the incident field this additional contribution to the scattered field generated by volume scattering of the tangential $\underline{E}_{o\omega}$ field component can be preponderantly greater than

[1] By this is signified the Rayleigh limit of Mie-Scattering; M. Born and E Wolf Principles of Optics, Chapt.13, Pergamon Press, New York, 1959.

that arising from the oscillating surface charge reacting to the normal component of the incident $\underline{E}_{0\omega}$ field, the Rayleigh-Mie field. Correspondingly, the incident field energy is more effectively dissipated due to the (particle) volume distributed Ohmic heating.

Given the efficiency in reradiation absorption associated with the (volume) scattering of the tangential field incident on a metallic particle of dimensions less than skin depth, radar absorbing technology offers a relevant class of applications. Because of the size of the individual particles, high particle densities still offer negligible weight penalties in loading or synthesizing low permittivity background dielectrics with a resultant dielectric constant or permittivity that is calculable by the Clausius-Mosotti[2] Lorentz-Lorenz[3] formula.

---

[2] Jackson, J.D., Classical Electrodynamics , Sect. 4.6, John Wiley and Sons Inc., New York, 1962.
[3] Reference 2, Chapter 2.

This study consists of 7 Tasks or Sections the objectives of which are summarized below.

1. DIELECTRIC PROPERTIES OF DISTRIBUTIONS OF SMALL CONDUCTORS

Establishes a more rigorous derivation of the dielectric properties of distributions of small conducting particles giving rise to the coherent absorption (and reflection) showing a sensitivity to particle size.

1.1 Metallic Particle Internal Field and Polarization

Develops a general theoretical treatment of the submicron metallic particle scattering problem giving rise to an effective particle polarization. This includes the classical (Mie) boundary condition matching theory extended to include volume scattering by conduction electrons in the limit of particle size less than skin depth. Volume scattering concerns collisional plasma dynamics and includes anomalies and modifications arising out of high incident field thresholds, low particle size to electron mean free path ratios, magnetic fields, and particle shape factors.

1.2 Composite Permittivity

Composite dielectric properties of dilute distributions of submicron metallic particles. Given the particle polarizability, establishes the permittivity for dilute concentrations imbedded in a uniform dielectric medium, recourse to classical constitutive relations for dilute mixtures, Lorenz - Lorentz, Clausius-Mosotti formulas, etc.

2. CONDITIONS FOR HIGH RADAR ABSORPTION

Studies in detail the conditions for high radar absorptivity in terms of types of metals, metal particle size range, particle number density range, tolerable non-uniformity in particle distribution, tolerable particle concentration gradient, radar wavelength range, and supporting dielectric materials for metal particles that can be used for high radar absorption.

3. BANDPASS CHARACTERISTICS

Investigates precisely the bandpass (absorption) characteristics of a finite thickness of absorber volume with a given metallic particle size. Studies vulnerability of the absorptive chaff function in terms of its passive microwave and both passive and active optical signatures.

4. DIELECTRIC MATERIALS

Surveys available dielectric materials to assess suitable radar-transparent candidates that can be loaded with submicron metallic particles to achieve high absorptivity and to satisfy component requirements for low Mach number aircraft at intermediate and low altitudes.

5. MASS REQUIREMENTS

Determines the required weight of submicron metallic particles for a specified volume of the atmosphere and supporting dielectric materials.

6. PREPARATION STORAGE AND DISPERSAL

Reviews, analyzes, and prescribes the preparation and storage of required submicron metallic particles and dispersal kinetics of the

particles in the atmosphere as a function of altitude and in the supporting dielectric materials. Discusses the lifetimes of the metallic particles in the atmosphere as a function of altitude and in the supporting dielectric materials.

7. EXPERIMENTAL VERIFICATION

Outlines initial experiments for the determination of necessary parameters to verify the concept developed theoretically. Makes a cost estimate for necessary experiments.

REFERENCING OF APPENDIX DERIVATIONS

The above Sections are decomposed into subsections with appropriate headings. Theoretical derivations are included in the Appendices and are correspondingly referenced at the end of each relevant subsection.

1. DIELECTRIC PROPERTIES OF DISTRIBUTIONS OF SMALL CONDUCTORS

1.1 Metallic Particle Internal Field and Polarization

1.11 Integral Equation Formulation for Internal Field

Literature review[3,4,5] and analysis have led to the establishment of an integral equation formulation of vector wave scattering by a small conducting particle of arbitrary shape, of critical dimensions less than the skin depth of the incident cw radiation. The integral equation must rigorously satisfy Maxwell's equations including the full boundary conditions for the electro-magnetic fields interior to the scatterer, and consistent far-field scattering generated by the effective current density sources. The approach taken is based on the vector Green's Theorem, or version of the classical Stratton-Chu integral formulation[4,5,6,7] extended to include induced surface charge. The following integral equation is a consequence of the formulation depicting the electric field vector $\underline{E}$ as the superposition of induced current and charge density $\underline{j}$ and ρ respectively.

$$\underline{E} = -\int dr' \left\{ \frac{i\omega}{c^2} \mu \underline{j} \psi - \rho \nabla \psi \right\} + \underline{E}_0 \qquad (1)$$

The particle dimensions are small, the largest dimension ranging from much less than the free space wave length to less than skin depth, and the smallest dimension less than skin depth. The essential properties considered in detail for such small particles are

3) Ref 1 Sect 2.4, 4) Ref 2 Sect 9.6,5) J.A. Stratton and L. Chu, Phys. Rev. 56, 99, 1939

6) Silver S., Microwave Antenna Theory and Design, Rad Lab Series 12. Sects 3.8-3.11, McGraw Hill, New York 1949.

7) Kleinman, R. Low Frequency Electromagnetic Scattering in Electromagnetic Scattering edited by P. Uslenghi, Academic Press, New York, 1978.

a Internal field is predominantly static zone.

b Interplay of incident tangential field vs induced surface charge produces net effective field driving the conduction electrons. Here particle shape properties will modify the respective field components.

c Because of the small dimensions the internal field is approximately constant amplitude. Estimates of the deviation from constant value are established by perturbation expansion of the interval field integral equation.

A basic requirement in the analysis is a careful correspondence with Rayleigh-Mie Theory in order to identify possible points of departure. The integral equation (1) for vector wave scattering by a small Rayleigh size conducting particle of submicron dimensions describes the internal electric field as arising from three interrelated sources: the incident field, the volume generated field produced by the driven conduction current, and the opposing Coulomb field of the induced surface charge. Here the derived integral equation with assumptions a, b, c, displays a novel form which permits direct physical interpretation of the depolarizing field for electromagnetically isotropic materials as dependent on the average solid angle subtended at the interior by the portions of the particle surface that are normal to the incident field.

$$E_p = -\frac{i\omega}{c^2}\mu\sigma\int d\underline{r}' E_p \psi + i\frac{\sigma}{\omega}\int dS_z' E_p \partial_z \psi + E_o \qquad (2)$$

where the polarization of $\underline{E}$ is along the z axis and

$$\psi = \frac{e^{ik_o R}}{R} \simeq \frac{1}{R} \quad , \quad R = |\underline{r} - \underline{r}'|$$

Then it follows that for $\underline{E}_p$ constant on the inner surface ...

$$E_p \simeq -\frac{i\omega\mu}{c^2}\int d\underline{r}'\,\frac{E_p}{R} + \frac{i\sigma}{\omega}E_{ps}\int dS_z\,\partial_z\left(\frac{1}{R}\right) + E_o \qquad (3)$$

Note that the depolarizing factor P_e is

$$P_e \equiv \int dS_z\,\partial_z\left(\frac{1}{R}\right) = \int dS\,(\underline{e}_z\cdot\underline{n})\,\underline{e}_z\cdot\nabla\left(\frac{1}{R}\right)$$

Surface component normal to $\underline{e}_z \quad dS\,(\underline{e}_z\cdot\underline{n}) = dS_z$

Solid angle subtended by $dS_z = dS_z\,\partial_z\left(\frac{1}{R}\right) = d\Omega_e$

Hence, the depolarizing field is shown dependent on particle shape in a simple, explicit way. The case for a spherical particle of submicron diameter, less than skin depth, is directly solved for the interior field by perturbation theory to first order in the volume current contribution.

$$E_p = \left\{1 - \frac{i\sigma}{\omega}\left(P_e - \mu k_o^2\hat{\epsilon}\right)\right\}^{-1} E_o \qquad (4)$$

$$\left.\begin{aligned} P_e &= \int dS_z\,\partial_z\left(\frac{1}{R}\right) = \frac{4\pi}{3} \\ \hat{\epsilon} &= \int d\underline{r}'\,\epsilon(r') \quad \leq \frac{4\pi}{3}r^2 \end{aligned}\right\} \text{ for sphere}$$

The result coincides with the Rayleigh-Mie solution, but with a small spatially varying volume current correction. It verifies that the integral equation formulation is indeed consistent with Rayleigh-Mie theory, in the limit of vanishing particle size, with explicit identification of the finite size corrections. [Appendix Section A1]

1.12 Spheroidal Particles

The case for non-spherical Rayleigh particles has then been investigated using ellipsoidal shapes where at least one dimension is submicron. Each component of the internal field that lies along an ellipsoidal axis is then formally derived in the same manner as in the spherical case, but its explicit evaluation depends on an elliptic integral for the depolarizing factor displaying the departure from sphericity.

$$E_k = \left\{ 1 - i\frac{\sigma}{\omega} \left(P_e(k) - \mu k_0^2 \hat{\epsilon} \right) \right\}^{-1} E_{0k} \tag{5}$$

$$P_{e_k} = 2\pi \int ds \frac{a_1 a_2 a_3}{(s+a_k^2)^{\frac{3}{2}}(s+a_j^2)^{\frac{1}{2}}(s+a_i^2)^{\frac{1}{2}}} \tag{6}$$

The cases of a spheroid or ellipsoid of revolution have explicit closed form expressions for the depolarizing factor. Define the eccentricity e_s in terms of the major, minor axes, a_1, a_2, $a_1 > a_2$ respectively. $e_s = \left(\frac{a_1^2 - a_2^2}{a_1^2} \right)^{\frac{1}{2}}$.

prolate spheroid, $P_e'(1) = \frac{4\pi}{e_s^2}(1-e_s^2)\left[\frac{1}{2e_s} \ln\left(\frac{1+e_s}{1-e_s} \right) - 1 \right]$ (7)

oblate spheroid, $P_e'(1) = 2\pi\left(1 - \frac{1}{e_s^2}\left[1 - \left(\frac{1-e_s^2}{e_s^2} \right)^{\frac{1}{2}} \sin^{-1} e_s \right] \right)$ (8)

As indicated in the general form of the internal field integral equation (for isotropic materials) the depolarizing factor is effectively proportional to the average solid angle subtended by that portion of

the particle surface that is normal to the incident electric vector. Thus a long thin rod will have an orientation which offers small depolarization, similarly will a thin flake. This is borne out by the appropriate limiting values of the depolarizing factor for prolate (rod) and oblate (flake) spheroids.

For $\frac{a_2}{a_1} \ll 1$, (7) becomes

prolate (rods) $$P_e'(1) \simeq 4\pi \left(\frac{a_2}{a_1}\right)^2 \ln\left(\frac{a_1}{a_2}\right) \qquad (9)$$

oblate (disks) $$P_e'(1) \simeq \pi^2 \frac{a_2}{a_1} \qquad (10)$$

As in the spherical case a small spatially varying perturbation correction to the depolarizing field contribution for the interior field is determined in terms of the induced volume current. These results indicate corroboration with Rayleigh-Mie theory and its more extentions of thin filament and thin flake theories, p.e. Greenberg[8], Kerker[9], Swinfo.[10] with further perturbation corrections displaying finer structure volume reradiation effects. It is to be mentioned that the depolarizing effects of geometric shapes may be amplified or reduced by electromagnetic anisotropy (multiply refractive crystal structure), a topic discussed by Kerker[9].

---

[8] Greenberg, M., Focusing on Particle Shape, Light Scattering by Irregularly Shaped Particles, D. Scheuerman, Ed, Plenum Press, New York, 1979.

[9] Kerker, M. Scattering of Light ... , Chapt 10, Academic Press, New York, 1969.

[10] Swinford, H, Electromagnetic Behavior of Radar Absorbing Chaff (RAC). Technical Note 354-43, June 1975, Naval Weapons Center, China Lake, California 93555.

The general solution is then established for the forward propagating internal field of a Rayleigh/submicron size conducting ellipsoid of arbitrary orientation relative to the incident plane polarized microwave field. The resultant field vector consists of the internal field components projected along the incident field direction.

$$\langle E_k \rangle = \left\{ 1 - i\frac{\sigma}{\omega}\left(P_e(k) - \mu k_0^2 \hat{\epsilon} \right) \right\}^{-1} E_0 \langle \cos(\underline{e}_z, \underline{e}_k) \rangle \quad (11)$$

$$= \frac{1}{3}\left\{ 1 - i\frac{\sigma}{\omega}\left(P_e(k) - \mu k_0^2 \hat{\epsilon} \right) \right\}^{-1} E_0 \quad (12)$$

Averaging over all orientations gives rise to one third the sum of the three depolarized field components derived for each alignment of an ellipsoidal axis with the incident field.

The formulation thus developed leads directly to the treatment of distributions of dipole scatterers comprising an artificial dielectric medium. [Appendix-Section A2]

1.13 Polarizability of Non-Magnetic Particles

The polarizabilities of three basic particle shapes, sphere, rod and flake, are derived using the integral equation formulation in which the depolarizing field is depicted as depending on the average solid angle subtended at the particle interior by the portions of its surface that are normal to the incident field. The resultant depolar-

izing factors in (7), (8), giving rise to internal field cancellation effects, are consistent with established results for non-magnetic conductors. They imply size ratios for negligible depolarizing effects consistent with (9), (10) cf

$$\text{rod} \quad \frac{a_2}{a_1} \lesssim \left(\frac{f/\sigma}{\ln f/\sigma + \ln \ln f/\sigma} \right)^{\frac{1}{2}} \tag{13}$$

$$\text{flake} \quad \frac{a_3}{a_1} \lesssim \frac{f}{\sigma} \tag{14}$$

The particle polarizability $\underline{\alpha}$ is defined here as the electric dipole moment per unit particle volume per unit electric field (in contrast to the usual definition as total dipole moment per electric field)

$$\underline{\alpha} = (\alpha_1, \alpha_2, \alpha_3) = \frac{1}{\Delta V_p} \frac{1}{|\underline{E}_0|} \left(\frac{1}{i\omega} \int \underline{J} \, dV_p \right) \tag{15}$$

$$\alpha_k = \frac{\sigma}{i\omega} \frac{1}{\left(1 - \frac{\sigma}{i\omega} P_{0k} + \hat{\epsilon}_k\right)} \tag{16}$$

The limiting values of the spheroid depolarizing factors are summarized:

- small sphere - depolarization factor is a constant, corresponding to an average internal solid angle of $(4\pi/3)$
- flake or oblate spheroid - depolarization decreases with aspect ratio of thickness to diameter. For non-magnetic conductors ($\mu \simeq 1$) its threshold lower limit is of the order of square root of frequency to conductivity (esu-cgs), below this ratio the depolarizing effect is negligible.

- rod or prolate spheroid - depolarization has greatest decrease with aspect ratio, width to length goes as the square of frequency to conductivity - the square of the oblate, flake, case as geometry would imply.

It appears that, for a single small non-magnetic sphere, reduction in size to submicron dimensions offers little or no improvement in re-radiation efficiency over Rayleigh size particles. The Rayleigh-Mie theory still applies unless other particles are adjacent with inter-particle separation along the field tangential direction is of order of the particle diameter. That is, for an isolated particle, the surface charge density induced by the normal component of the incident field will cancel much of the tangential and internal field driving the conduction electrons, thus generating a weak internal current density. The presence of adjacent particles will neutralize or short circuit the induced surface charge and enhance the internal current, thus simulating the improvement limit for small aspect ratio flakes and rods. [Appendix-Sections A3 - A5, E]

1.14 <u>One and Two Dimensional Propagation Models - Absence of Depolarizing Field</u>

A side issue considering transition to lower dimensional wave propagation and scattering has been treated in Appendix F for the case of randomly distributed very long and thin parallel rods or films.. Here the induced depolarizing field is totally absent and the problem reduces to the scattering of an incident field by 2(rod) or 1(film)

dimensional plasma or metal "particles". The continuity of the tangential electric and magnetic fields then permits a direct Born perturbation series solution for the scattering amplitude of a single "particle", the counterpart to the 3D dipole moment. It is shown that the convergence condition requires the "particle" thickness be less than skin depth. [Appendix-Sections A5, E]

1.15 Conductivity Dependence on Particle Size

The effect of particle size on conductivity arises out of boundary or wall reflection enhancement of the electron momentum transfer collision frequency. This gives rise to the anomalous skin effect and the conductivity is a decreasing function of particle thickness to electron mean free path ratio. A literature survey and some supporting analysis has been carried out. Wilson[12], 1965, summarizes theoretical and experimental results for thin films and wires, extrapolations are being developed for spheres. The data indicates that reductions in conductivity of an order of magnitude for particle sizes of interest are to be expected.

1.16 Effect of High Incident Electric Fields

The electrical conductivity is a decreasing function of the effective collision frequency, primarily due to scattering by the thermally vibrating ions, with impurities, strains, etc. playing an important part at low temperatures. As a consequence, the conductivity values vary inversely with temperature, as T^{-1} to T^{-5} for normal to low temperatures respectively (Wilson[12]). The internal temperature

---

[11]) Ref. 9 Sect. 8.4.3,

[12] Wilson, A. H., Theory of Metals , Chapt. 8, Cambridge 1965.

is proportional to the thermal energy which is unaffected by low fields. However, as the internal field energy increases above the mean thermal energy, the effective temperature becomes porportional to the mean incident power. A threshold for the onset of this non-linear effect is determined by the so-called "plasma - field", described by Ginzburg[13] and others. For metals, this corresponds to fields of the order of 10^6 volts/cm. Because of the high electroconductivity, this nonlinearity in metals is almost unattainable in practice.

1.17 Highly Magnetic Conductors

Analysis has been carried out of the integral equation determining the electric field internal to a high μ conducting sphere of radius r upon which is incident a plane polarized electric vector. It is shown that a necessary condition for constant internal electric field is $r < \lambda / (2\pi\sqrt{4\pi\mu})$ λ free space wave length (esu, cgs)

When this inequality is violated the assumption of a constant internal field leads to contradiction. The physical significance of this posed condition is based on the high value of μ giving rise to a strong current-driven transverse field generated by and in opposition to the oscillating electrostatic depolarization field. Thus within a submicron thick layer of the order of the skin depth of a particle of Rayleigh dimensions, r,

$$\lambda / 2\pi > r > \lambda / (2\pi\sqrt{4\pi\mu}) \qquad (17)$$

conditions for cancellation of the depolarizing field should exist, giving rise to more efficient RF absorption.

[13] Ginzburg, V.L., Propagation of Electromagnetic Waves in Plasma, Chapt.8, Pergamon, New York, 1978.

1.18 Thin Layer Spherical Shells

A first order analysis has been carried out of the absorbing properties of thin layered, magnetically permeable, conducting spherical shells, and is extendable to spheroids. The shell radius r_s and thickness δr_s are assumed small enough for the internal field to remain constant. Hence the sphere is of modified Rayleigh size $r_s \lesssim \lambda/2\pi\sqrt{\mu}$ *. The shell thickness δr_s has two ranges of values:

- a trivial limiting value of $\delta r_s = r_s$, a solid modified Rayleigh scatterer, and
- $\delta r_s \lesssim r_s$, a very thin layer.

The latter case of a very thin shell signifies a correspondingly small internal depolarizing field, since the average solid angle subtended by the induced Coulomb field is small. As a result, the longitudinal (electrostatic, charge-generated) and transverse (electrodynamic, current-generated) fields are comparable and small. Therefore the incident and internal electric fields should not differ substantially. This is borne out by analysis. The integral equation for the internal field is solved as a perturbation about a constant value in a layer thin enough so that both transverse and longitudinal fields are small, with the transverse field exceeding the depolarizing field. The convergence condition for the thin shell approximation of a constant internal field requires that the shell thickness to radius ratio, $\delta r_s / r_s$, be of order of or less than one third of the square root of the frequency to conductivity ratio

$$\delta r_s / r_s \leq \sqrt{f/\sigma}/3 \qquad (18)$$

*The term modified Rayleigh used signifies the $\mu^{-\frac{1}{2}}$ reduction in size, unmodified Rayleigh thus refers to setting $\mu = 1$.

and thus, with the modified Rayleigh particle size requirement, leads to a shell thickness δr_s less than skin depth .

$$\delta r_s < \delta r_{s_R} = c/2\pi\sqrt{\mu\sigma f} \qquad (19)$$

Under this thin "Rayleigh" shell approximation the polarizability of a shell dipole is predominantly imaginary. [Appendix-Section A7]

1.19 Extended Analysis of Internal Electric Field Equation

A more comprehensive treatment of the electric field (wave) equation internal to the conducting particle has been develcped in Appendix A 7 to verify and sharpen the conclusions derived by the perturbation solution to the Stratton-Chu based integral equation that has been used. This latter integral equation form depicts the internal electric field as due to the sum of the incident field and the reaction fields arising from the induced surface charges and volume currents. The more detailed treatment assumes the Rayleigh condition, namely particle size much less than free space wave length. The internal field wave equation is homogeneous, source-free, with the medium described by its complex permittivity. By choosing an orthogonal coordinate system in which the wave equation is separable and where the "radial" coordinate is constant on the particle boundary (ellipsoidal shapes are assumed), the problem simplifies to one dimension with a homogeneous solution requiring two arbitrary constants. One of these constants is eliminated by requiring finiteness of the solution at the origin.

Interior Equation

$$(\nabla^2 + k^2) E = 0 \tag{20}$$

with solution $$k^2 = \frac{\omega^2}{c^2}\left(1 + i\frac{4\pi\sigma}{\omega}\right)$$

$$E = C\,\mathcal{E}(\xi) \tag{21}$$

where $\mathcal{E}$ is finite at ellipsoid origin, and boundary shape defined by $\xi = \text{const.}$

The second constant is specified by substitution of the homogeneous solution into the Stratton-Chu integral form relating the various incident and induced field contributions. This leads to the boundary integral equations

$$0 = \frac{-1}{4\pi}\int dS\left(\partial_n \psi \underline{E} - \psi \partial_n \underline{E}\right) + \frac{i\sigma}{\omega}\int d\underline{S}\cdot\underline{E}\,\underline{\nabla}\psi + \underline{E}_0 \tag{22}$$

Substantiation of (23) in (24) results in the value of constant C as

$$C = \left\{\left(1 + \frac{i\sigma}{\omega} P_e\right)\mathcal{E}(\xi_s) - \left(\int dS \frac{1}{R}\right)(\partial_\xi \mathcal{E})_s\right\}^{-1} E_0 \tag{23}$$

This method has the advantage of identifying the functional behavior of the internal field. Generally for large particles an infinite set of constants is necessary since the field is not essentially a function of one variable, but the Rayleigh smallness condition reduces this to the one dimensional, tractable form.

The analytical results indicate that the internal field at the inner boundary of the particle is closely approximated by its small radius limit. But this inner surface value exponentially decays with a skin-depth pennetration distance, reaching its minimum at the center. This quantitatively describes the expected result of a surface layer (particle size permitting) of skin depth thickness in which the penetrating field is

absorbed. The material bounded by the penetration layer is ineffective, hence offers "excess weight". However, the penetrating field can be very small due to surface scattering when the spheroidal particle has a large depolarizing factor. [Appendix-Section A7]

1.110 Spheroidal Metallic Shells, Negligible Depolarization

A thin spheroidal shell of thickness less than skin depth, as described previously, offers negligible scattering with the additional requirement that the depolarizing factor of the shell be small. For spherical shells, this small depolarization condition requires a thickness to radius ratio δ_{rs}/r_s less than the frequency (esu, cgs) to conductivity ratio ω/σ, that is

$$\delta_{rs}/r_s \angle 3\omega/4\pi\sigma \quad , \quad \omega = 2\pi f\,(\text{Hz.}) \qquad (24)$$

For spheroids, the ratio would be more like

$\delta_{rs}/r_s \angle \omega/P_e\sigma$, for P_e the depolarizing factor of the spheroid.

In addition to very high aspect ratio (length to thickness) conducting rods and disks, thin shelled conductors also offer high absorption efficiency. But they offer obvious practical difficulties in manufacturing and structural stability.

1.111 Metallic Coating of Ultrafine Dielectric Particles

However, the deposition of submicron metallic layers on fine, non-conducting, particles is a developed technology. Various methods are available for the metal coating of fine dielectric particles. As early as 1963[14] the coating of fine particles for industrial applications has been a topic of R&D. Techniques include chemical precipitation methods, metal spraying or condensing metal vapor. Investigation of the fine particle coating methodology is being pursued and will be discussed further.

Thus for small metallic coated particles of non-conducting material, scattering is predominantly due to reradiation by the net induced charge across dielectric discontinuities while absorption is associated with the resistive Ohmic heating loss of the resultant internal field within the metal layer. With a very thin metallic layer, less than skin depth, and a small depolarization factor within the layer, the maximum field penetrates and correspondingly maximizes the absorption.

---

[14] Loftman, K.A., Coatings Incorporating Ultra Fine Particles, Ultra Fine Particles, Eds Kuhn, Lamprey and Sheer, Wiley, New York, 1963

1.112 Conclusions On Metal Layered Spheroids

The following summarizes the results of recent analyses

- Rayleigh particles considered, $r_s \ll \lambda_0/2\pi\sqrt{\mu}$, conductors
- Absorption of internal field within a layer of skin depth thickness

If particle dimension r_s $>$ skin depth $\rightarrow$ excess mass

$\leq$ skin depth $\rightarrow$ max absorption of depolarized internal field.

extinction cross section,

$$\frac{\sigma_e(r)}{\sigma_e(r = \text{skin depth})} = \frac{\text{mass of absorbing layer}}{\text{mass of particle}} \approx \frac{\text{skin depth}}{\text{particle size}}$$

- Metal coated dielectric-insulator particles:
  Metal layer acts as absorber. If metal layer thickness less than skin depth, have appreciable transmission through layer, hence appreciable absorption. A distribution of such particles represents Rayleigh dielectric scatters plus absorbing skin depth layered shells. For a dilute distribution, absorption effects predominate.
- High μ (ferromagnetic) layers:
  Allows much smaller thickness, mass, for the same effect.

Restrictions on metal layer thickness:

If the metal layer is too thick, for its surface curvature, the layer depolarization factor can be appreciable, thus diminishing the internal field and the absorption. The layer thickness to shell radius ratio

$\delta r_s / r_s \leq 3\omega / 4\pi\sigma$ suffices for negligible polarization within the spherical shell. For non-spherical, i.e. spheroidal shells

$\delta r_s / r_s \leq \omega / P_e \sigma$

is expected, P_e = depolarizing factor.

It then follows that magnetic particles can have

$\delta r_s \leq \omega r_s / P_e \sigma$ = skin depth = $c/(2\pi\sqrt{\mu\sigma\omega})^{(cm.)}$

Thus maximum absorption is achievable since the entire incident field is absorbed. [Appendix Section A8, A9]

1.113 Internal Field Spatial Dependence

The internal field spatial dependence on the dominant radial coordinate was determined for limiting cases of Rayleigh-size spheroids of submicron thickness. The wave equation for the interior electric field was approximately solved as an ordinary differential equation in the dominant coordinate. Finiteness at the origin and substitution into the Stratton-Chu equation form to match boundary conditions then

permitted evaluation of the arbitrary constants of the solution.

The functional forms of the solutions are summarized [Appendix-Section A8]

TABLE 1 FUNCTIONAL FORMS OF RADIALLY DEPENDENT FIELD SOLUTION

Solid Particle Shape \ Property	Limiting Radial Coordinate	Internal Field Form
Sphere	Radius	$C\ (\sin kr)/r$
Oblate spheroid disk	Thickness	$C' e^{ikx}$
Prolate Spheroid rod	Thickness Radius	$C'' J_0 (k\rho)$ Zero order Bessel function

for k = effective propagation vector magnitude in the medium.

The spatial behavior indicates an exponential attenuation of the depolarized field at the surface, extinction within a skin depth δr_{sk} penetration

$$\delta r_{sk} \simeq Im\left(k^{-1}\right)$$

1.114 Thin Shell Approximation, Depolarizing Factors

The depolarizing factor for any Rayleigh-size particle has been derived as the average solid angle subtended within the particle volume by the induced electrostatic surface charge. Thus for the depolarizing factor of a thin layer, the solid angle integral is subjected to a small variation along the surface normal. The results then refer to a layer of thickness δr_s, much less than the curvature radius of surface, $\delta r_s / r_s$. The ratio of the layer depolarization factor, δP_e, to

the factor for solid particle, P_e is then proportional to the relative thickness of the layer $\delta v_s / v_s$. More specifically, a summary is presented in the following Table 2.

TABLE 2 LIMITING DEPOLARIZING FACTORS OF SOME SHELL SHAPES

Shell Shape	P_e (solid)	δP_e (layer)
Sphere	$4\pi/3$	$8\pi/3$
Oblate Spheroid disk	$\pi^2(a_2/a_1)$	$\pi^2(\delta r_s/a_1)$
Prolate Spheroid rod	$(2\pi \ln 2)\ (a_2/a_1)^2$	$(2\pi \ln 2)(a_2/a_1)(\delta r_s/a_1)$

where a_2 = minor axis, a_1 = major axis, $a_2/a_1 \ll 1$

It is seen that for sufficiently small depolarization, in the case of a spherical shell the only recourse is a very thin layer since $P_e = 4\pi/3 = \text{const.}$

For the spheroids, higher aspect ratios denote lower depolarizing factors (in the direction of the smaller axis). Thus the depolarizing factor of a thin spheroid layer has two "degrees of freedom", the aspect ratio of the spheroid shape, and the layer thickness. This signifies that higher aspect ratio spheroids require less stringent conditions on the layer thinness for acquiring negligible depolarizing factors. The most relaxed conditions apply to the prolate spheroid.

The reduction of the depolarizing factor denotes that penetration of the incident electric field strength is undiminished by surface charge induction. However, the limiting penetration depth is still the skin

depth of the particle or layer. Spheroidal layers of thicknesses greater than skin depth absorb less efficiently per unit mass since the attenuated field negligibly affects the inner layer conduction electrons. [Appendix-Section A10, A11]

1.2 Composite Permittivity

1.21 Permittivity Formulation

A general formulation is established for the composite dielectric constant or permittivity and resultant power reflection coefficient of dilute concentrations of varities of submicron sized metallic particles imbedded in a low permittivity medium. Slab geometry has been considered. [Appendix-Section B1-B3]

1.22 Composite Permittivity

Coherent forward scattering over a band of wavelengths is of interest so that the mean separation between particles must be less than a quarter of smallest wave length (in the supporting medium).

The classes of particle shapes considered in a general mixture are: submicron spheres, submicron thin prolate spheroids or filaments and oblate spheroids or disks. The latter spheroids have varying depolarizing factors.

Dilute concentrations of each particle shape class, namely, volume fractions much less than unity, are assumed. The net polarizability of each species is then established, and, with the corresponding volume fractions, the Clausius-Mosotti-Lorenz - Lorentz expression for the effective permittivity ϵ is then developed for the mixture. It is given expression in terms of the conventional rational fraction form

of the weighted average of species polarizabilities, $\bar{\alpha}_k$.

$$\epsilon = \frac{1 + \frac{4\pi}{3} \sum_1^3 F_k \bar{\alpha}_k}{1 - \frac{4\pi}{3} \sum_1^3 F_k \bar{\alpha}_k} \tag{25}$$

$$\bar{\alpha}_k = \frac{1}{3} \sum_{j=1}^{3} \alpha_k(j) \qquad \alpha_k(j) = \frac{i\sigma}{\omega} \frac{1}{\left(1 + i\frac{\sigma}{\omega} P_{e_k}(j) + \hat{\epsilon}_{j,k}\right)}$$

k = particle species, particle of volume ΔV_k

j = j^{th} axis parallel to incident $\underline{E}_o$ vector, j = (1, 2, 3)

$F_k = N_k \Delta V_k$ = Volume fraction of K^{th} species. [Appendix Section B4]

1.23 Power Reflection/Absorption

The Fresnel based power reflection coefficient R for slab geometry is then established to account for "first reflection" effects due to the discontinuity in refractive index, from free space to the substrate plus dipole mixture. For normal incidence

$$R = \left| \frac{\sqrt{\epsilon} - 1}{\sqrt{\epsilon} + 1} \right|^2 \tag{26}$$

The power transmission coefficient is then one minus the reflection coefficient for an absorbing medium of sufficient length. Absorption is implied if there is an imaginary part to the composite refractive index, the square root of the corresponding dielectric constant (this is equivalent to the dielectric constant having a negative real part or an imaginary part). The absorption is an Ohmic heating effect and, thus refers to an extinction depth within the absorbing medium. The effect of dilute concentrations of non-absorbing scatterers in the

composite medium is to increase the absorption slightly, due to the correspondingly reduced group velocity associated with the real refractive index. [Appendix - Section B4]

2. CONDITIONS FOR HIGH RADAR ABSORPTION

2.1 Principal Contributors to Absorption

The contributions of the various species to the overall power absorption can then be directly identified from

$$\epsilon = \frac{1 + \frac{4\pi}{3}\left(\frac{i\sigma}{3\omega}\frac{F_1}{(1+i\delta_1+\epsilon_1)} + \left\langle\frac{1}{P_{e_2}}\right\rangle F_2\right)}{1 - \frac{4\pi}{3}\left(\frac{i\sigma}{3\omega}\frac{F_1}{(1+i\delta_1+\epsilon_1)} + \left\langle\frac{1}{P_{e_2}}\right\rangle F_2\right)} \qquad (27)$$

where

F_1 denotes volume fraction of all particles with very small depolarizing factor components

$(P_e)_1 = \delta_1 \leq \omega/\sigma$

and F_2, $\left\langle\frac{1}{P_{e_2}}\right\rangle$ refer to volume fraction and mean reciprocal depolarizing factor of particles with greater depolarization

$(P_e)_2 > \omega/\sigma$

The most efficient absorbers are those with lowest depolarizing factors. Thus filaments and disks with high length or diameter to thickness ratios produce the dominant absorption. Spherical particles which are electrostatically isolated from each other, with minimum separation distances of several diameters have a large, constant, depolarizing factor of $4\pi/3$, and thus absorb inefficiently as Rayleigh scatterers. However, analysis of the electrostatic coupling between adjacent spherical particles has been carried out. [Appendix Section B3]

2.2 Depolarization Reduction Due to Close Electrostatic Interaction

The physical situation concerns the cancellation of the depolarization field of a spherical dipole due to induced interacting fields from adjacent particles. A linear array of dipole spheres, aligned with the incident electric vector, and with arbitrary separation distance between pairs of sphere centers, was investigated to determine the mean effective depolarization field at the interior of any one sphere. First order results indicate that a mean separation between centers of a little over a diameter would cancel the depolarization effect. This is an expected result since the linear array forms a string of particles simulating a filament. Correspondingly it indicates an obvious way of generating filaments from linear clusters of submicron particles. Similar conditions obtain for two dimensional arrays, simulating disks or flakes. The thickness of the clusters must remain of submicron-dimensions for RF in order to permit tangential field penetration. [Appendix - Section E]

2.3 Linear Filaments or Planar Disks as Submicron Clusters

Submicron spheres arranged in linear or planar clusters will then produce the optimum absorption because of their negligible depolarization field. The maximum dimensions of these respective clusters are then given by the corresponding values for the actual filaments and disks [9,10] (Kerker, Swinford).

2.4 Resonance Absorption

The power absorption coefficient for normal incidence and planar slab geometry in the case of optimally or resonant absorbing filaments

or clusters take a particularly convenient form as a simple function of the dimensionless variable, β, as the product of the volume fraction and ratio of conductivity to frequency (cgs-esu) for resonance absorption of type 1 particles

$$\epsilon = \frac{1+2i\beta}{1-i\beta} \qquad \beta = \frac{4\pi}{9}\frac{\sigma}{\omega}F_1 = \frac{2\sigma}{9f}F_1 \tag{28}$$

extinction depth x_d

$$x_d = \frac{\lambda}{2\pi \mathcal{I}_m \sqrt{\epsilon}} \tag{29}$$

- Power reflection coefficient R
- absorption coefficient 1-R
- absorption or extinction depth to wavelength ratio $\frac{x_d}{\lambda}$

are summarized in Figure 1 which indicates absorption for a high conductivity metal would require a volume fraction (A>99%) of 10^{-4} at 10 GHZ, with an extinction cross section per particle volume of 10^7 and absorption thickness of .5 cm. [Appendix-Section B5]

2.5 Shell Distribution Reflection/Transmission

The conventionally formulated mean dielectric constant or electric permittivity is established for a concentration of spherical shells uniformly distributed in radii and of thicknesses less than the skin depth of the highest frequency in the band width of the incident field. The resultant permittivity indicates reflection/transmission coefficients of slab geometry that compare with the resonant conditions of long filaments or thin flakes, i.e. such dilute concentrations of particle

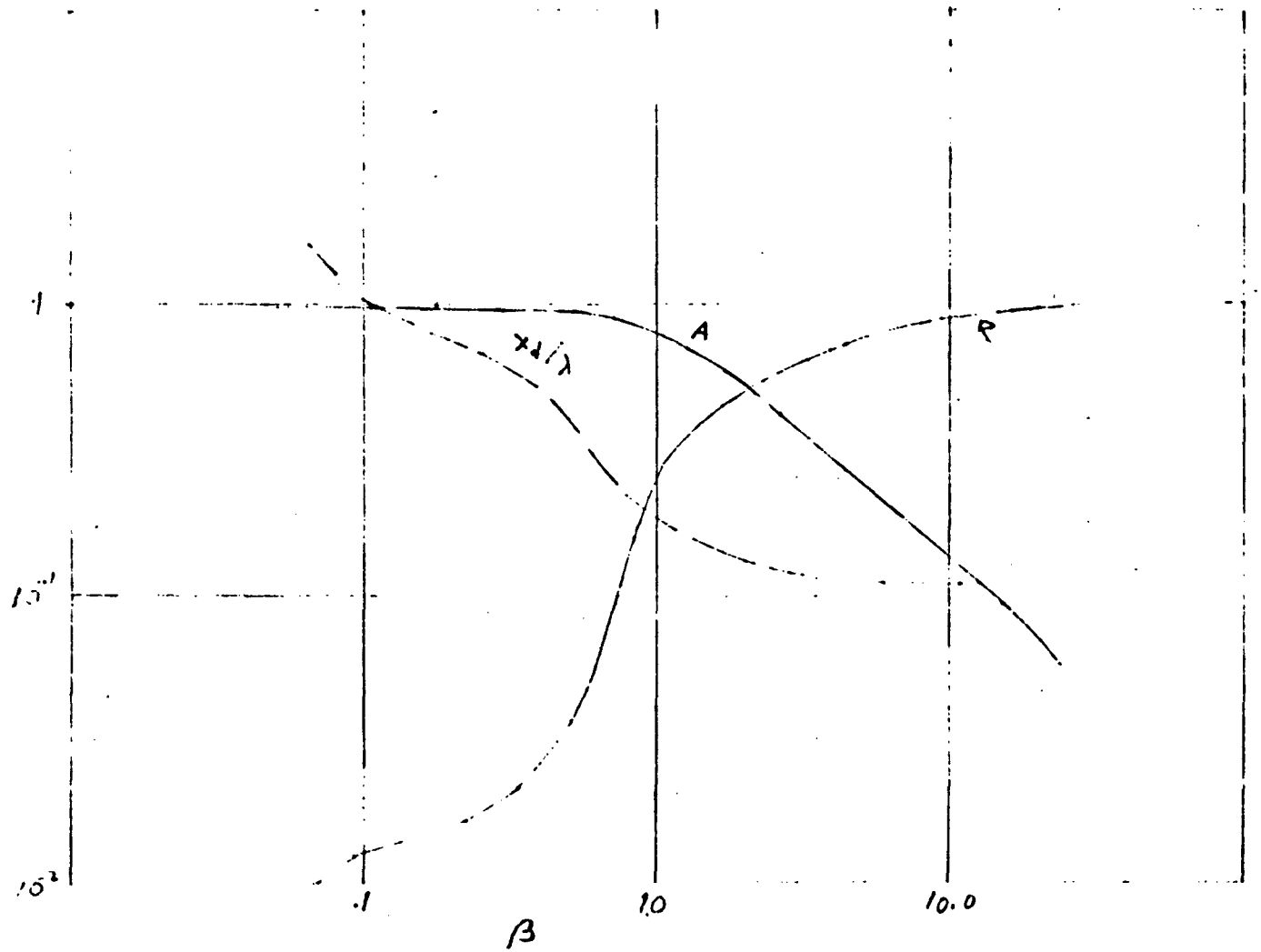

Figure 1. Power Reflection/Absorption of Efficient Absorbers vs β

shells produce virtually the maximum attainable absorption. This is to be expected since depolarization is negligible in the shell. The problem is that of realizing such thin conducting shells, essentially small tenuous metallic "bubbles". [Appendix-Section A10, B5]

2.6 Application to Solid Magnetic Conducting Spheres

A suboptimal result is associated with more easily manufactured solid spheres or spheroids. It concerns the thin outer absorbing layer of magnetic conductors over which the incident field is constant, unmodified Rayleigh size particles in the sense that $r_s < \lambda/2\pi$. But because of the permeability μ* conditions permit the predominance of the tangential over the induced, depolarizing, fields within a skin depth size layer δr_{sk}. Beyond this layer the tangential field becomes negligible, the inner core depolarizes and substantially cancels the incident field. The particle size requirements for this layer absorption are

$$\lambda/2\pi\sqrt{\mu} < r_s < \lambda/2\pi \qquad (30)$$

Thus highly magnetic ($\mu \gg 1$) particles can be of very small size and still absorb. This outer layer thickness is estimated by the shell model and the composite permittivity is determined now for "fatter" scatterers with an inner core that scatters purely Rayleigh. The absorption is still high but efficiency is reduced by the preponderant mass of the unmodified Rayleigh core. The amount of mass of solid sphere required to produce a given high percentage of absorption now is increased over the shells by a factor of the order of $\sqrt{\frac{\sigma}{f}}$.

Thus for small, high μ particles, appreciable absorption may take place

* μ is the AC permeability $\mu(f)$ that must be considered as indicated in Sect. 4.2.

over a broad band which can extend to the optical region. Conditions for this merit investigation.

3. BANDPASS CHARACTERISTICS

3.1 Broad Band Effects, by a Composite Dielectric Slab

Consider the band pass characteristics of a composite dielectric consisting of a dilute concentration of spheroidal conducting particles of conductivity σ (sec^{-1} , esu cgs) which display this negligible depolarizing factor "resonance" at an RF frequency f_0 (Hz). These particles may be assumed high aspect ratio disks or rods. Thus shell or layer counterparts, as well as spherical layers are assumed supported by non-conducting cores. The particulate distribution is supported in vacuum, or in a dielectric substrate of high transparency.

In order to formulate a broad band absorber, over frequencies, $f_1 < f_2$, from a distribution of such resonant depolarizing scatterers, the following requirements are necessary.

- Mean particle depolarizing factor, say $\bar{P}_e$, must be of order of or less than ratio of lowest in-band frequency to conductivity.

  $$\bar{P}_e \lesssim 2\pi f_1/\sigma$$

  (This will eliminate electrostatic depolarization).
- Representative particle or layer thickness δr must be of order of or less than skin depth δr_{sk} of highest band frequency

  $$\delta r \leq \delta r_{sk}(f_2)$$

  (Maximizes absorption to mass ratio)
- Length of dielectric "slab" must be greater than longest wave length of band of interest, corresponding to the longest extinction depth of the attenuating medium.

3.2 Band Edge Definition

a) High frequency edge $f > f_2$

In this case, the constituent particles of the composite dielectric have thicknesses greater than skin depth. As the penetration depth approaches and exceeds skin depth the net tangential electric field, which is the dominant component, undergoes cancellation, eventually giving rise to purely "elastic" non-absorptive scattering by the Rayleigh dipole, (still in the Rayleigh-size regime). The effect of tangential field cancellation is expressed to first order as a down scaling of the volume fraction of scatterers, F, by the ratio of skin depths δr_{sk} as

$$F(f)/F(f_2) = \delta r_{sk}(f)/\delta r_{sk}(f_2) = (f_2/f)^{\frac{1}{2}} \quad (31)$$

Hence for a particle size $rs < \delta r_{sk}(f_2)$, a frequency of $f \geq 2f_2$ will result in an attenuation reduction of

$$\frac{\text{DB attenuation } (f)}{\text{DB attenuation } (f_2)} = \left[\frac{f_2}{f}\right]^{\frac{1}{2}} \quad (32)$$

b) Low frequency edge $f < f_1$

The lower frequency limit on effective absorption signifies the onset of dominant depolarizing effects. The lower limit f_1 must fulfill

$$f_1 \geq \sigma \bar{\rho}_e$$

where $\bar{\rho}_e$ is the lowest depolarizing factor, associated

with propagation along a spheroid thickness or shape direction. The extinction depth for in band frequencies is independent of frequency. For a frequency $f \angle \sigma \bar{P}_e$, depolarizing is significant and absorption is weak with an extinction depth that depends on wave length. The ratio of extinction depths χ_d "in band" to lower frequencies is

$$\frac{\chi_d(f_1)}{\chi_d(f)} = \frac{\bar{P}_e^2 \sigma^2}{4\pi^2 f^2} \qquad f \angle \frac{\bar{P}_e \sigma}{2\pi} \leq f_1 \tag{33}$$

Thus lower frequency components can tunnel through the optically thin slab medium. If we set the lower band frequency f_1 at the depolarizing threshold

$$f_1 = \bar{P}\sigma/2\pi$$

The attenuation A of frequencies f lower than f_1 tends to follow the relationship

$$(A(f))_{DB} = 23(f/f_1)^2 \tag{34}$$

Thus a reduction of 50% below f_1 will result in a degradation in attenuation effectiveness of 6 DB.

3.3 Summary of Absorption Band Requirements

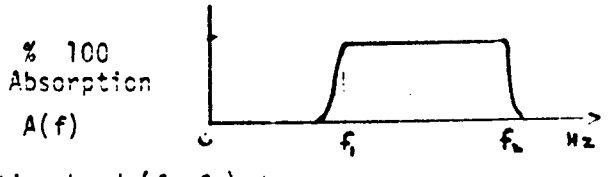

Absorption band (f_1, f_2) Hz.

metal (particle) thickness $\leq$ skin depth of highest frequency $= \frac{c}{2\pi\sqrt{2\sigma\mu f_2}}$

particle concentrations $\beta(A > 95\%) = \hat{\beta}$

$$\beta = \frac{2\sigma}{9}\frac{F_1}{f} \qquad \beta_{max} < \hat{\beta}$$

or $F_1 < \frac{9}{2\sigma}\hat{\beta} f_1$ volume fraction

Slab length $L_D > \lambda_1 = \frac{3c}{2\pi F_1 \sigma}$

Absorption Band Edges

a) $f_2 < f$ $\qquad A(f) = \left(\frac{A(f_2)}{100}\right)^{(f/f_2)^{-\frac{1}{2}}} \times 100$

b) $f_1 > f$ $\qquad A(f) = \left(\frac{A(f_1)}{100}\right)^{(f/f_1)^2} \times 100$

3.4 Reflection Considerations

When the negligible depolarizing factor condition is maintained and concentrations allowing coherent effects are assumed, the composite medium power reflection coefficient, for normal slab incidence is an increasing function of the dimensionless parameter $\beta = \sigma F_c / 2\pi f$, F_c, the volume fraction of the absorbing metal. In reference to Figure 1. High reflection, greater than 95%, occurs for values of β greater than 10; while greater than 95% absorption arises for β less than 1.

3.5 Band Width Requirements (f_1, f_2)

For reflection, the requirements are similar to absorption as far as the skin depth - particle size condition on the highest frequency f_2 is concerned.

An increase in frequency resulting in a decrease in skin depth thickness also reduces the reflection efficiency, expressible as a reduction in

the effective volume fraction of scatterers.

The lowest frequency f_1 also refers to an extinction depth, but this is the effective skin depth $(\delta r_{sk})_{eff}$ of the composite medium, much less than the slab length L_s.

$$\max (\delta r_{sk})_{eff} \leq L_s \tag{35}$$

$$L_s \geq \sqrt{2}\, \lambda_{max} \tag{36}$$

since the dielectric constant approaches - 2. A reduction of reflection by 20%, from 95% to 75%, for example, arises from a frequency increase of 2.5 times the upper limit f_2 taken as $\sigma \bar{P}_e$.

3.6 Optical Frequency Considerations, Incoherent Scattering

Because optical frequencies are orders of magnitude greater than RF, the condition for negligible depolarization $\bar{P}_e \leq 2\pi f/\sigma$ has a smaller upper bound. The condition for Rayleigh scattering requires particles with largest dimensions in the submicron range, and thicknesses one or two orders of magnitude smaller. Coherent effects further requiremean particle separation of less than 1/4 wave length, unrealistic number densities of 10^9 or higher. Hence incoherent scattering effects are much more realizable for optical frequencies.

Corresponding to the skin depth for coherent scattering is the Beer law extinction depth for the incoherent case. This is the depth within which the total scattering cross section matches the beam frontal area[15] [16] [17]

[15] Van de Hulst, H. Light Scattering by Small Particles, Chapt 19, Wiley. New York, 1957

[16] Reference 1 Chapt 13.

[17] Swinford H. and W. Cartwright, A Short Derivation of the Absorptive Scattering Properties of Short Filamentary Chaff, N.W.C. Technical Memorandum 3718, March 1979, Naval Weapons Center, China Lake, California 93555.

When depolarization is negligible the scattering loss is absorptive (Swinford '79) and a dilute concentration of 10^3 to 10^4 particles / cc will require an absorption thickness of a few centimeters for wavelengths from 1 to 10 μm. Otherwise, with large depolarizing effects, a compensating increase in number density by a factor of greater than 10^3 would be necessary to keep the same thickness. For constant number density, the slab thickness must be correspondingly increased.

3.7 Passive Signatures, Radiometric Emission

R.F.: For resonant depolarizing particle sizes, the active conditions for high absorption and reflection over a band $f_1 < f_2$ H_z correspond to the passive conditions of high and low emissivity. The one-way active extinction and composite slab skin depths then correspond to the optical thicknesses of the emitting media.

Optical: The incoherent scattering properties of concentrations of resonant particles have been discussed above. For this class of particle, the composite medium is absorptive and thus radiates at the mean temperature of the constituent particles (and dielectric substrates) within an extinction depth thickness.

Given conditions for active coherent R.F. reflection or absorption over a band $f_1 < f_2$ GH_z in terms of "resonant" or efficient absorbing particle sizes, concentrations, and slab thickness. Since the particle sizes are assumed too large for optical "resonance" penetration, the passive optical signature of the particles is easily shown to be insignificant with the only optical radiometric contribution arising from the dielectric substrate. Thus in a near vacuum the radiometric temperature of such a particulate cloud is purely background.

4. DIELECTRIC MATERIALS

4.1 Radar Transparent Dielectrics

A review of technical and commercial literature has been undertaken to assess radar transparent dielectric material that can be loaded with submicron metallic particles or metal layer granules to achieve high absorptivity and satisfy component requirements for low Mach number aircraft at low and intermediate altitudes.

The frequency range 1 to 30 GHZ has been considered for radar transparent materials. Materials providing low loss tangent, less than .0003, with sufficient rigidity for experimental testing of principle, and for use in operational aircraft are polyeurethane - polystyrene based, and are commonly used by manufacturers. Emerson and Cuming, Canton, Mass. is very well known in the technology and has been taken as typical.[18] The dielectric constants lie in the range 1.02 to 1.1 implying 99.5% to 97% transmission. The technique of producing so-called artificial dielectrics by loading pure dielectric material of refractive index matched to air by small particulates has been well established for radar reflectors and lenses, while development of radar transparent materials has been essential for use in all weather radomes and for streamlined radomes of high speed missiles and aircraft. For strength to support air loads a thin radome is supported by a low dielectric constant ($K < 1.1$) polyeurethane foam, that serves to hold a radar reflector (ECCO Reflector Trademark). A typical design is described as capable of withstanding velocities of Mach 2 for several minutes. At velocities of Mach 3 and above, ceramic radomes and ceramic foams would be necessary.

[18] Luoma, E, ECCO REFLECTOR BROCHURE, Emerson and Cuming, Inc., Canton, Mass., 1976

The extinction lengths, extinction cross-sections and mass requirements for high absorption have been summarized.

4.2 High Permeability Effects for Weak Incident Fields

Sufficiently high permeability of some ferromagnetic conductors can amplify the absorption efficiency by significantly reducing the extinction depth requirement. While the conductivity of some non-magnetic metals, p.e. Al., Cu, exceeds that of the ferromagnetic types, the product $\mu_{eff}\sigma$ determines the effective particle polarizability, as a result high μ^*_{eff} composites predominate in absorption efficiency. But this amplification effect applies to weak incident fields, far below the saturation limit of the absorbing particle, where the incident magnetic field linearly drives the magnetic induction. Thus the absorbing particles must be remotely located from the RF microwave source, as in radar applications. The most efficient solid shape is the prolate spheroid or rod of low aspect ratio, thickness to length of less than 10^{-3} for non-magnetic conductors. This stringent aspect ratio can be relaxed for high μ_{eff} materials, translating into aspect ratios of $\sqrt{\mu_{eff}} \times 10^{-3}$.

---

* Composite Permeability μ_{eff}

Except for determining the skin depth, the particle polarizability is relatively insensitive to μ, however in a concentration of high μ particles, the overall effect on extinction or absorption is related to the product of the effective medium permeability μ_{eff} and conductivity, σ $\mu_{eff}\sigma$. Thus the improvement in absorption, over a non-magnetic conducting particle with the same conductivity, is obtained by replacing σ by $\mu_{eff}\sigma$.

This μ_{eff} is the composite permeability of the medium, however, and not the specific μ of the ferromagnetic metal.

4.3 A.C. Ferromagnetic Permeability $\mu'(f)$

It is also the case that ferromagnetic materials display the greatest frequency dispersion in permeability for microwave frequencies[19]. One interpretation of this dispersive effect is that at some critical frequency, the direct action of the field will be opposed by the eddy current field so that movement of the domain boundary is limited[20]. Thus the D.C. μ undergoes some modification and reduction. However, fine particles comprised entirely of single domains, of micron or less dimensions display high A.C. permeability that may be comparable to the D.C. value.

4.4 Form of Permeability Factor

Thus the static permeability μ must be replaced by $\mu(f)$ its microwave counterpart. The effective permeability μ_{eff} of a distribution of low depolarizing or demagnetizing factor particles then is

$$\mu_{eff} = \frac{1 + \frac{8\pi}{3} F\mu(f)}{1 - \frac{4\pi}{3} F\mu(f)} \qquad (P_e << 1)$$

---

[19] Bozorth, R., Ferromagnetism, Chapts. 17, 18, Var Nostrand, New York 195[illegible]
[20] Kittel, C. Theory of Structure of Ferromagnetic Domains, Phys. Rev. 70, 965-71.

4.5 Metal Coated Spheroids

Highly efficient absorption can also arise from distributions of metal coated ultra-fine dielectric particles, where the relative thickness of the metal layer is sufficiently small to eliminate the internal depolarizing field, while the absolute thickness is less than the metal skin depth. Because of the larger spatial volume occupied by a spherical shape, the extinction depth is also correspondingly larger, in comparison with lower aspect ratio spheroids, however the mass requirements remain small. Ferromagnetic metal coatings can only improve the efficiency by reducing the extinction depth for all layer shapes.

4.6 Dielectric Loading

In the case of dielectric loading, a permittivity of less than 2 for the dielectric will produce less than 5% reflected power at normal incidence. Polystyrene is one example with a very low density of .05 gms/cm^3.

5. MASS REQUIREMENTS

The extinction lengths, $\frac{\text{extinction cross section}}{\text{particle volume}}$ and mass requirements for high absorption have been summarized.

The following Tables 3 and 4 offer a brief summary of the absorption properties of various particle distributions, both, parametrically (Table 3), and for specific materials, aluminum and iron (Table 4):

The symbols and terms used in Table 3 and Table 4 are defined -

(cgs - esu - Gauss units are used)

F	volume fraction, F_m metal layer, F_p particle
μ_{eff}	effective magnetic permeability = $\hat{\mu} \leq (1 + \frac{8\pi}{3} F\mu(f)) / (1 - \frac{4\pi F\mu(f)}{3})$
σ	conductivity
c	light speed
P_e	depolarizing factor
ρ	density, ρ_m metal, ρ_f dielectric core
$\delta r/r$	relative thickness of layer
$\mu(f)$	A.C. ferromagnetic permeability.

Extinction depth x_d

$$x_d(\lambda) = \lambda / (2\pi \mathrm{Im}\sqrt{\varepsilon})$$

$$\left(\frac{\text{Extinction Cross Section}}{\text{Particle Volume}}\right) = F/x_d$$

Mass requirements for greater than 95% absorption over a frequency band, f_{min} to f_{max} (Hz) $= \rho F x_d(\lambda_{max}) \times 10^4$ gms/M^2

The term "resonant" is used to denote limiting low thickness to length aspect ratio for negligible depolarization, $P_e < 10^{-3}$

SUMMARY TABLE 3 - ABSORPTION PARAMETERS - (f_{min} to f_{max} H_z)

Absorbing Particle	Extinction Length	Extinction Cross Section per Particle Volume	Mass Requirements	Thickness Requirements
	cm	cm^{-1}	gms/cm^2	
Resonant Disks (Oblate Spheroids)	$\frac{3c}{4\pi\hat{\mu}\sigma F}$	$\frac{4\pi\hat{\mu}\sigma}{3c}$	$\frac{3c\rho}{4\pi\hat{\mu}\sigma}$	particle thickness less than skin depth = $\frac{c}{2\pi}\frac{1}{\sqrt{2\mu(f)f_{max}}}$
Resonant Rods (Prolate Spheroids)	$\frac{3c}{2\pi\hat{\mu}\sigma F}$	$\frac{2\pi\hat{\mu}\sigma}{3c}$	$\frac{3c\rho}{2\pi\hat{\mu}\sigma}$	
Non-resonant Rods	$\frac{3c\sigma P_e^2}{2\pi\hat{\mu}\omega^2_{min}F}$	$\frac{2\pi\hat{\mu}\omega^2_{min}}{3c\sigma P_e^2}$	$\frac{3c\sigma P_e^2\rho}{2\pi\hat{\mu}\omega^2_{min}}$	
Non-resonant Disks	$\frac{3c\sigma P_e^2}{4\pi\hat{\mu}\omega^2_{min}F}$	$\frac{4\pi\hat{\mu}\omega^2_{min}}{3c\sigma P_e^2}$	$\frac{3c\sigma P_e^2\rho}{4\pi\hat{\mu}\omega^2_{min}}$	
Metal Coated Spherical Particles	$\frac{\lambda max}{\pi F_p}$	$\frac{\pi\hat{\mu}}{\lambda max}$	$\frac{\lambda max}{\pi\hat{\mu}}\left[3\rho_m\frac{\delta r}{r}+\rho_f\right]$	$\frac{\delta r}{r}=\frac{3\omega_{min}}{\sigma}$
Metal Coated Spheroids-Rods	$\frac{6c\sigma P_e^2}{\pi\hat{\mu}\omega^2_{min}F_m}\left(\frac{\delta r}{r}\right)$	$\frac{c\pi\hat{\mu}\omega^2_{min}}{6c\sigma P_e^2}\left(\frac{r}{\delta r}\right)$	$\frac{6c\sigma P_e^2}{2\pi\hat{\mu}\omega^2_{min}}\left(\frac{\delta r}{r}\right)\left[\frac{\rho_m\delta r}{r}+\rho_f\right]$	$\frac{\delta r}{r}<\frac{3\omega_{min}}{8\pi P_e\sigma}$
Metal Coated Spheroids-Disks	$\frac{3c\sigma P_e^2}{\pi\hat{\mu}\omega^2F_m}\left(\frac{\delta r}{r}\right)$	$\frac{\pi\hat{\mu}\delta^2_{min}}{3c\sigma^2P_e^2}\left(\frac{r}{\delta r}\right)$	$\frac{3c\sigma P_e^2}{\pi\hat{\mu}\omega^2_{min}}\left(\frac{\delta r}{r}\right)\left[\rho_m\frac{\delta r}{r}+\rho_f\right]$	$\frac{\delta r}{r}<\frac{3\omega_{min}}{4\pi P_e\sigma}$

TABLE 4 - ABSORPTION BY NONMAGNETIC (Al)* AND FERROMAGNETIC (Fe)* CONDUCTING PARTICLE DISTRIBUTIONS

	Material	Particle Thickness (cm.)	X_d (cm^d)	Mass/Area > 95% A (Band .10 to 10.GHz) (gms/M^2)	
Resonant Rod	Al	10^{-4}	300	10^{-3}	
	Fe	2×10^{-6}	300	1.6×10^{-2}	
Non-Resonant Rod (Pe = .1)	Al	10^{-3}	3.5×10^{6}	7×10^{9}	Purely Rayleigh - Non-resonant Scattering/absorption Pe too high
	Fe	10^{-3}	10^{6}	7×10^{9}	
Metal Coated Sphere (Pe(core)= $\frac{4\pi}{3}$	Al	$\frac{\delta r}{r} = 10^{-4}$	300	5×10^{4}	Thin metal layer negligibly depolarized
	Fe	2×10^{-6}	300	5×10^{4}	
Metal Coated pheroid (Rod)	Al	$\frac{\delta r}{r} = 10^{-4}$	90	$.45\ Pe \times 10^{5}$	Pe of dielectric Core < 1
	Fe	2×10^{-6}	360	$Pe \times 10^{5}$	

*Nominal Values - Al: $\sigma \simeq 10^{17}\ sec^{-1}$, $\rho \simeq gms/cm^3$, $\mu_0 = 1$

Fe: $\sigma \simeq \frac{\sigma(Al)}{4}$, $\rho \simeq 8\ gms/cm^3$, $\mu = 5{,}000$

6. PREPARATION STORAGE AND DISPERSAL

6.1 Metal Coating Techniques

Ultrafine non-metallic particles of low density, coated with a thin-skin depth or less-layer of conducting metal, offer efficient RF microwave absorption. Coating techniques include chemical precipitation metal spraying or condensing metal vapor[14]. Of particular interest is the reduction of metals from solution by hydrogen and the extension of this technique to the metal coating of powders by the Sherritt process has been described in Reference [21]. In the case of nickel, which is also of higher magnetic permeability, it is indicated that the only materials that would be expected to be completely and evenly coated with metal (nickel) by hydrogen reduction techniques would be those that are as at least as effective as hydrogenation catalysts as the metal in question. The Sherritt process offers a surface activation treatment of nickel by establishing surface activation centers with water insoluble anthraquinone. This method has also been applied to the preparation of nickel coated glass.

6.2 Production of Non-Spherical Metal Particles[22, 23]

Micron size metallic particles are generally inefficient absorbers unless they form the constituents of filaments or flakes with very low depolarizing factors. Some methods of producing metallic dust particles give rise to filament or flake shapes as well as highly irregular surfaces which may offer substantially low depolarizing factor components. The following are among such methods -

[21] B. Meddings, W. Kunda, and V. Makiw, Preparation of Nickel Coated Powders, in Powder Metallurgy, W. Leszinski Editor, Interscience, New York, 1960.

[22] R. Dixon and A. Clayton, Powder Metallurgy for Engineers, Machinery Publishing Co. Ltd., 1971 (England)

[23] Bakensto, A., Commercial Methods for Powder Production, in Vol. 3. Iron Powder Metallurgy, Editors Hausner, Rolland, Johnson, Plenum Press, New York, 1968.

Atomization - a furnace melted precision fed atomizing jet stream.

Electrolytic Technology - electrolytic deposition of powder flakes that are easily crushed to powder.

Reduction of Oxides - reduces high grade (iron) magnetic concentrates, produces sponge iron - easily pulverized.

Mechanical Grinding - Used in manufacture of flake powder.

Hydrometallurgy - precipitation of metal powders from hydrogen.

6.3 Production of Fiber Sized Particles[24, 25]

Fiber shaped non-metallic particles that can be used as non-conducting cores for metal layer deposition can be generated from dust or powder by means of a vibrating fluidized-bed principle. The powder is placed into a vibrating cylinder (made of metal or glass) and dried gas is passed vertically through the powder layer, forming a fluidized bed. The aerosol generation is controlled by the equilibrium state developing between the disintegrating and reagglomerating of the powders or fibers in the surface layer of the vibrating bed. The vibration breaks the cohesion between the particles or fibers so that they are free to be carried away by the gas stream. This method permits dust clouds of constant concentration to be generated for periods of several hours or several days.

6.4 Acoustic Agglomeration of Aerosols[26]

The above method has some similarities to the method of acoustic agglomeration of aerosols where a fixed mass of powder is exposed to an acoustic pressure field. The number density of small aerosols decreases

[24] Spurny, K., Fiber Generation and Length Classification, in (6).
[25] Generation of Aerosols and Facilities for Exposure Experiments, K. Willecke, Editor, Ann Arbor Science, Ann Arbor, Mich., 1980.
[26] Shaw, D., Acoustic Agglomeration of Aerosols in Reference (25).

as the aerosol size increases by agglomeration while the total mass remains constant. Acoustic aerosol generation has been successful in the USSR by growth rate control. Both ultrasonic standing waves and progressive sawtooth waveforms of the order of 100 Hz have been effective.

6.5 Whisker and Filament Production[27]

The manufacturing of materials in the form of metal fibers, or whiskers, are of importance in metallurgical technology because of their exceptionally high mechanical resistance. These whiskers have a very high length to diameter ratio with diameters in the micron or submicron range and lengths of the order of meters. Hence by segmenting or controlled growth they can be the basis of production of resonant absorbing filaments or rods, Rayleigh size in length, skin depth in diameter. The technique of unidirectional solidification achieves in a single process the on site growth of fibers. These whiskers are based on a technique for the fabrication of continuous metal filaments with growth from the liquid state called EFG - "edge defined, film fed growth". They consist of continuous monocrystals with micron diameters and meter lengths.

6.6 Opposing Jet Classifier [28]

A jet of particle-laden air is directed against an equally strong axisymmetrically opposed jet of clean air. Higher inertia particles deviate across the air streamlines and cross the fluid interface between jets, while lighter ones are carried with the original air stream. Once separated, the two particle fractions can be directed to any desired location for further size classification.

This method provides -

[27] Piatti, G., Preparation of New Multi-Phase components, in Proceedings of the International School of Physics, Enrico Fermi, Course LXI, Edited by G. Caglotti, North Holland, 1978.

[28] K. Willecke and R. Pavlik, Opposing Jet Classification, in Reference 25.

. Sharp particle size separation above and below a desired aerodynamic cut size with both effluent particle fractions remaining in the airborne state.

. Permits extraction of narrow particle size range from a polydisperse aerosol cloud.

Present research is focussed on the suppression of the edgetone effect and the elimination of high particle losses for small separation plate hole sizes.

6.7 Dispersal Techniques [29]

Some dispersal techniques commonly used in pollutant health studies are

1) Dust Generators Utilizing Scrapers -

Here a scraper continuously slices particles from a container of powder, which may be compacted into a cake. A common device is the Wright dust feeder where the powder is compacted into a cup at fairly high pressures forming a hard cake. A geared mechanism rotates the cup across the scraper and an air flow entrains the scraped particles.

2) Fluidized Bed-Dust Generators -

- Fluidize dust material to be aerosolized.
- Fluidize mixture of larger inert particles and smaller dust particles.

[29] V. Marple and K. Rubow, -- Concepts and Parameters, in Reference 25.

The fluidized bed is comprised of the inert metallic particles. For a constant output from the generator the particles are transported from a powder holding chamber to the fluidized bed by a chain conveyor system driven by a variable speed motor which controls the dust quantity delivery.

6.8 Particle Storage and Aging

Stored particles in dielectric material may undergo change in their properties due to aging with time and chemical reactions with the material. Aging may be caused by oxidation and/or solid-solid diffusion. The oxidation and diffusion rates can be estimated if the composition of the dielectric material is known. The composition of most dielectric materials can be obtained from the manufacturers and the rate estimation could be made. If we take the Al particles because of their low density, the oxidation rate of Al, which is fast, needs to be compared with the desired lifetime of theirs in the dispersed cloud. If the lifetime desired is larger than the oxidation time, the particle needs to be coated to slow down oxidation.

6.9 Agglomeration Prevention

Techniques of the particle preparation have been described previously and not repeated here. The small particles of some metals may agglomerate easily due to cold welding effect. For example, pure aluminum particles agglomerate easily under pressure, but if they are coated with a thin (a few tens of Angstroms) layer of aluminum oxide they would not agglomerate easily for the same conditions. Various coatings can be used to prevent agglomeration but not to change their absorptive properties. For example, a metallic particle coated thinly with a non-reactive teflon would minimize agglomeration. The particles in an appropriate liquid medium will remain dispersed. Thus, agglomeration can be prevented by various techniques and

the most suitable technique can be evaluated analytically and then followed by experiments.

6.10 Dispersal Kinetics of Aerosol Sized Particles[30] [31]

In the dispersal of micron sized metal particles by means of the free expansion of a sustaining (inert) gas under pressure in the manner of aerosol ejection, two simple physical models apply

a) Isothermal expansion of sustaining gas in vacuum or near vacuum conditions.

b) Adiabatic expansion of sustaining gas.

a) Isothermal Expansion in Near Vacuum Conditions

Here the ambient pressure is negligible, hence the thermal energy of the sustaining gas remains constant as its density decreases through expansion. Thus the number of momentum transfer collisions imparted to a particle moving in steady state with respect to the flow is proportional to the local gas density. The equation of particle mass conservation or continuity then establishes the inverse square relationship for the evolved density ρ at a radial distance r sufficiently far from a localized emitting source of density ρ_0 of dimension r_0

$$\rho = \rho_0 \frac{r_0^2}{r^2} \quad , \; r \text{ indefinitely large}$$

b) Adiabatic Expansion of Sustaining Gas in Ambient Atmosphere

This applies to atmospheric conditions. The sustaining gas expands isentropically to ambient pressure conditions (displaying some hydrostatic buoyant behavior) and achieves a finite confining volume to the particle distribution as a limit to the expansion mode. A single pulse source of initial density P_0 volume V_0 and pressure P_0 will then expand to a volume

[30] N. Fuchs, and A. Sutugin, Highly Dispersed Aerosols, Chapt. 9, Ann Arbor Science Publishers, Ann Arbor, Mich., 1970.

[31] Brock, J. The Kinetics of Ultrafine Particles, Aerosol Microphysics I, Particle Interaction, Ed. W. H. Marlow, Springer Verlag, New York, 1980.

and density

$$V = V_o\left(\frac{P_o}{P}\right)^{\frac{2}{3}}, \quad \rho = \rho_o\left(\frac{P}{P_o}\right)^{\frac{2}{3}}$$

A sequence of pulses of constant over pressure will result in a time increasing particle concentration within the confining volume, given by setting $\rho_o = \dot{\rho}_o t$. Loss of particles in the volume V is due to a slower diffusion process, thus, in order to maintain a steady concentration of particles, the rate of emission must balance the diffusion rate. Because of the enormously greater mass of the solid particle it is expected that the diffusion loss would be very slow, requiring small incremental corrections to the emitted output.

6.11 Analysis of Mass Requirements for Absorption

Parametric analyses have been carried out to formulate the mass requirements or mass rate requirements for the maintenance of a high degree of RF - microwave absorption at high altitudes.

- Idealized Model - Spherically Symetric Source (Within given solid angle)
- Radially Symmetric number density o
- Require Transmission at R_1 to be less than 1%
- Leading edge of density wave at R_2
- Because of $1/R^2$ dependence of density transmission at R_1 IF $R_2 >> R_1$ ($R_2 = 10\ R_1$) is same as transmission at $R_1 = R_0$ with uniform density from R_1 to R.

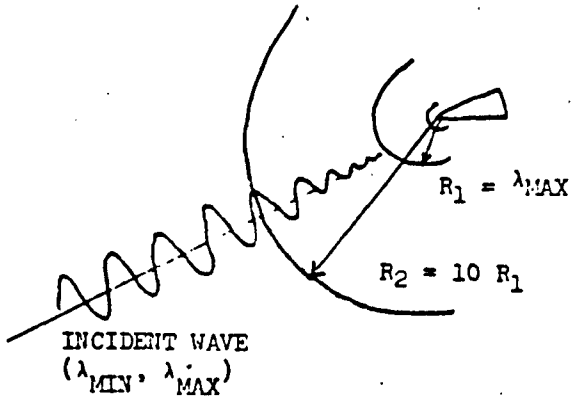

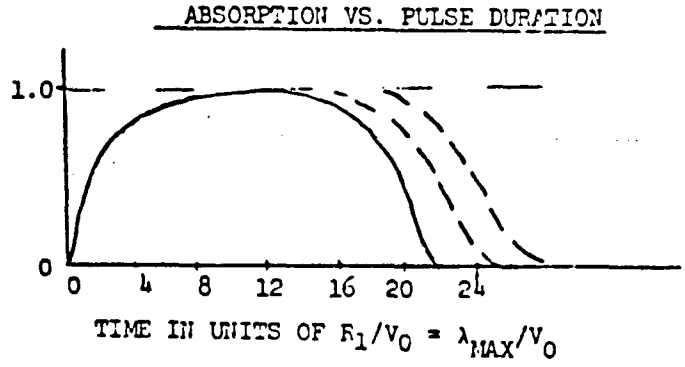

Figure 2.- Deployment Parameters Near-Vacuum Aerosol Dispersion

Figure 3.- Absorption vs Pulse Duration Effectiveness

The following summarizes the ideal limit in deployment parameters/aerosol properties for the first order model described.

TABLE 5 SUBMICRON METAL AEROSOL CONCEPT EFFECTIVENESS SUMMARY

FREQUENCY BAND	PARTICLE SIZE (resonant rods)	ABSORPTION LENGTH	MASS REQUIREMENTS (>90% ABSORPTION	
			MINIMUM	TOTAL MASS (1000 SEC. V_0 = 1 fps = .3 MPS
X-L	$< 1.3 \times 10^{-5}$ CM	30 CM	15×10^{-3} GMS	15 GMS
L-VHF	$< 4 \times 10^{-5}$ CM	3000 CM	489 GMS	900 GMS
X-VHF	$< 1.3 \times 10^{-5}$ CM	3000 CM	489 GMS	900 GMS

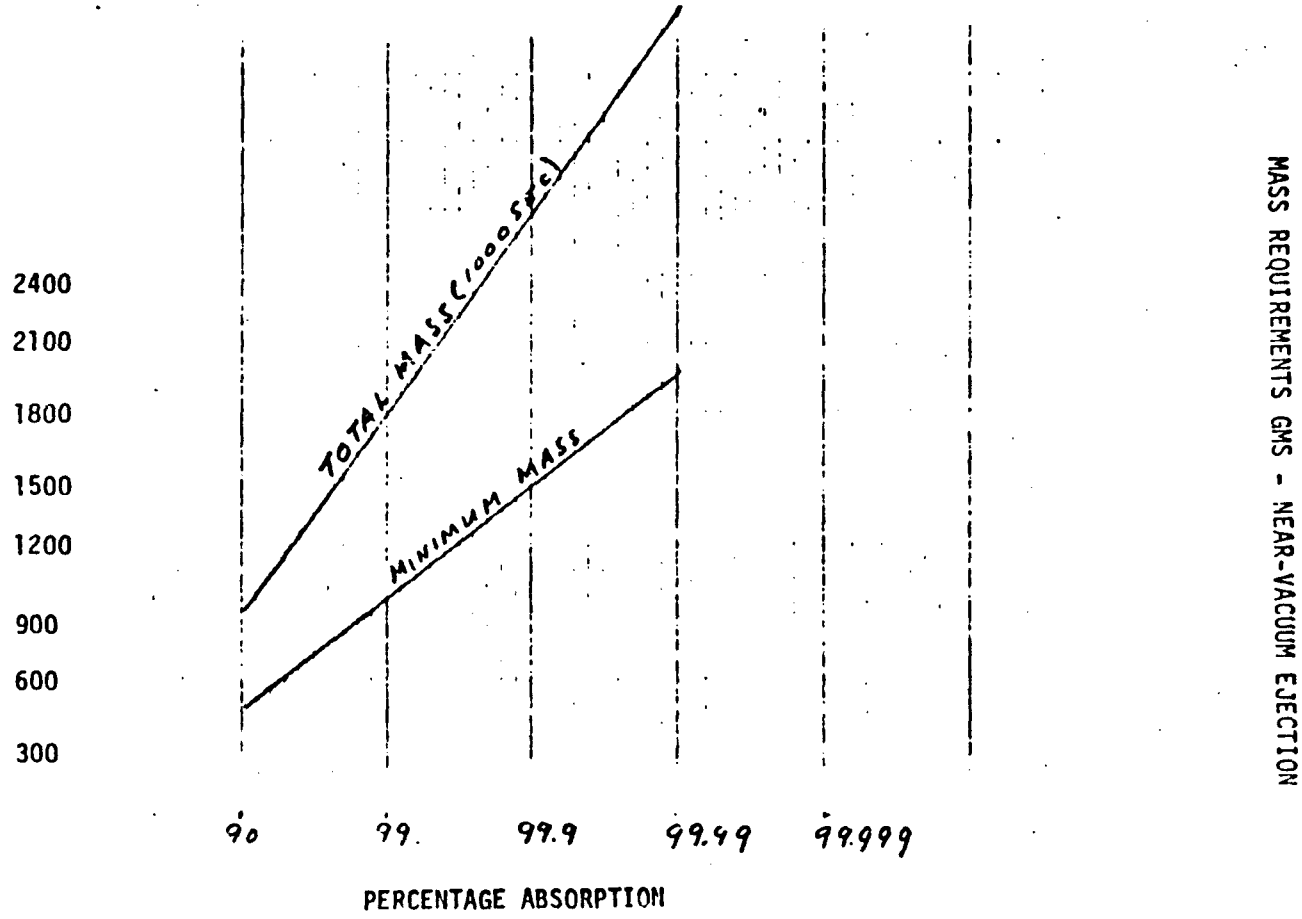

Figure 4. Ejected Mass Requirements vs, Percentage Absorption

7. EXPERIMENTAL TESTING

The simplest, first order approach is recommended for test of principle, the measurement of the power reflection and transmission coefficients of a dielectric plate before and after loading with dilute concentrations of particles. The frequencies concentrations, particle shapes and particle constitutive properties are prescribed by the theoretically predicted requirements for efficient absorption. Shape classes include very low aspect ratio solid metal (aluminum) filaments and flakes, moderate aspect metal coated spheroids, including spheres, of low permittivity dielectric cores . . polystyrene or polyeurathane for example. Ultrafine particles or layers of ferromagnetic metals of very high permeability (iron, permalloy) should also be tested.

A typical experimental configuration[32] for RF measurements entails a dielectric plate "window" between shielded enclosures. Transmission and reflection measurements can then be made for a discrete set of RF frequencies. Basic calibration of the maximum dynamic range is obtained with the window entirely open, and with it closed by a totally reflecting metal plate. The frequency range is from 0.1 to 10 GHz. The costs for experiments or measurements are expected to average $600. a day, and a week of testing should be considered.[32]

Similar smaller scale measurements can be carried out by standard broadband microwave network reflection measurements[33].

[32] Parker W.H., GENISTRON RFI/EMI ANALYSIS CAPABILITIES, Genisco Technology Corp., 1981.

[33] Lance, A. Introduction to Microwave Theory and Measurement Systems, McGraw Hill, New York, 1964.

Another well-known organization in the field of research development and manufacturing of radar absorbing dielectrics[18] has quoted* preliminary estimates for the generation and testing of the desired loaded dielectric plates. The dielectric base would be a low permittivity dielectric such as polystyrene or polyeurathane of K < .1 in the GH_z range. The generation of several plates 1 or 2 feet square with different recipes, i.e. solid filaments, solid flakes, metal coated spheroids, would cost in the vicinity of $10,000. Free Space measurements are preferable and are routine for them with costs of $100 per sample/per frequency, with the maximum frequency range of .1 GHz to 10 GHz. For a first order test of the principles a more practical band of 2 to 3 GHz could suffice, with perhaps discrete frequencies of .1 GHz separation.

*E. Luoma, Chief Physicist, Emerson and Cuming Corp., Canton, Mass., has offered this information in private communication, 13 August, 1981.

SUMMARY AND CONCLUSION

The internal field of a Rayleigh conducting particle is depolarized at its inner boundary, with the depolarizing factor equal to the average internal solid angle subtended by the component of the incident electric vector that is normal to the particle surface. Thus spheres have a constant depolarizing factor of $4\pi/3$, while ellipsoids, and (analytically more tractable) spheroids of very low minor to major axis - aspect ratios can have very low depolarizing factors. The depolarizing factor dependence with small aspect ratio prolate spheroids or rods varies as the square of the aspect ratio, while for oblate spheroids, it varies directly with the aspect ratio.

The depolarized inner boundary field then is skin depth attenuated within the particle, the inner core remaining unaffected and offering excess weight. With one or more dimension less than skin depth in the submicron size range for RF-microwave, the internal field can be substantially constant and the volume power absorption to mass ratio or absorption efficiency maximized for the given deplolarizing factor. Thus suitably oriented submicron particles with negligibly small depolarizing factors, of the order of or less than the conductivity to applied frequency ratio (esu cgs) offer the most efficient absorption since virtually all of their conduction electrons participate.

The absorption properties of Rayleigh sized spheroidal metal shells are sim' in principle to the solid particles. The metal shell or layer surrounds a low permittivity (near free space) light weight spheroidal shaped solid dielectric. The thin shell signifies a reduction in subtended solid angle, within the metal layer, from that of the solid spheroidal shape.

For the shell, the depolarizing factor of the underlying spheroid shape is multiplied by the shell thickness to semi major axis ratio. Thus the more stringent requirements on solid particles for negligible depolarizing factors, requiring aspect ratios of less than 10^{-3} (rods) to less than 10^{-6} (disks) are reduced for their thin shell counterparts since higher aspect ratio dielectric cores can be used. On assuming a shell layer thickness of a micron, the required depolarizing factor for a prolate spheroid should be numerically less than its semi major axis, while for an oblate spheroid less than one percent of the semi major axis is the numerical upper bound on the depolarizing factor.

For high permeability ferromagnetic materials the conclusions are similar to the non-magnetic case. However, for efficient absorption the Rayleigh size criterion must be reinterpreted to its modified form requiring a reduction in the conventional Rayleigh dimension bound by the reciprocal square root of the permeability. This is necessary in order to prevent the large eddy current induction from cancelling the incident field under low depolarizing geometries. The skin depth condition for efficient absorbing still applies, with the proper inclusion of permeability in the skin depth expression. Thus the particle dimension or layer dimension may be appreciably smaller than submicron.

The presence of neighboring particles acting as electrostatic dipoles has been shown to produce a negligibly neutralizing effect on the depolarizing field except for high concentrations, with inter-particle separation of the order of particle diameter.

Non-linear effects due to high internal fields are unlikely for good conductors because of the very high electron plasma field that must be surpassed.

Particle size effects on conductivity can be significant when the dimensions are exceeded by the conduction electron mean free path in the metal. For submicron dimensions the rise and persistence of incoherent wall scattering effects would reduce the conductivity of a typical metal particle to one tenth of its bulk value.

The composite permittivity of dilute concentrations of metal and metal-layered spheroidal particles has been established through the conventional Clausius-Mosotti, Lorentz-Lorenz formulation - the determination of the mean polarizabilities, dipole moments and consequent polarization of the particle distribution. In the case of efficient absorbers, the Fresnel power reflection coefficient for slab geometry and normal incidence is a function of the dimensionless variable - the ratio of the product of conductivity and volume fraction to applied frequency. Under these conditions the required volume fraction of efficient aluminum like absorbers for greater than 95% reflection is of order of or less than 10^{-6}, while for greater than 95% absorption a volume fraction of less than 10^{-8} is required. For absorption by dilute distributions the extinction depth is comparable to the wave length of the incident field.

The following conclusions apply to absorption band requirements for a dilute slab distribution of efficient absorbing particles. For greater than 95% absorption in the band from a minimum of f_1 to a maximum of f_2 Hz:

. The particle thickness should be less than the skin depth of the highest frequency.

. The maximum wave length λ_1, should be less than the slab thickness.

Frequencies higher than f_2 will not penetrate the particles hence the net tangential field will tend to zero, wave lengths greater than λ_1 will tunnel or leak through the entire slab.

Beyond the absorption band edges (f_1, f_2) the attenuation decay (or transmission rise) is sharply defined, with a steeper decay at the upper frequency f_2.

For reflection band considerations over (f_1, f_2) the higher concentration of efficient absorbers gives rise to a sharp jump in the magnitude of the relative permittivity toward the value -2, resulting in high percentage reflection.

. The high frequency f_2 condition on particle size is similar to the absorption case.

. The low frequency f_1, condition, is imposed by the requirement that the effective slab skin depth be somewhat greater than the maximum wave length λ_1, again, to prevent tunneling.

The passive RF-microwave signature of the composite dielectrics, used for absorption or reflection is black body radiation at the temperature of the particles concentrated within the extinction depth or skin depth of the slab distribution.

The optical signature of such composite dielectrics is predominantly dependent on the optical scattering and emissive properties of the supporting dielectric substrate. The optical back scatter cross-section is roughly the

sum of the individual particle areas for Mie scattering hence, of the order of -10 to -20 DBSM. The passive optical signature of the metal particles is virtually negligible.

Radar transparent dielectric materials are available for loading and experimentation with operational manufacturing and testing techniques in standard practice. Polyeurathane - polystyrene based materials offer low loss tangent, very close to free space permittivities, light weight and sufficient rigidity for experimental testing. The weight requirements for typical dielectric substrates such as polystyrene are of the order of 5 kgms per square meter for absorption of 1 GHZ or higher frequencies.

Distributions of ferromagnetic conductors can improve absorption efficiency by significantly reducing extinction depth requirements, provided that the effective permeability of the distribution is high. This requires efficient size particles, of low depolarizing or, demagnetizing, factors that retain a high A.C. permeability, achievable through selection of particle sizes of magnetic domain dimensions or less, in the submicron range.

The extinction lengths, extinction cross sections and mass requirements for efficient absorbers (referred to as resonant absorbers), as well as inefficient ones of high depolarizing factors, have been summarized parametrically and for the specific cases of aluminum and iron. The solid shapes requiring minimum mass are oblate spheroid disks of aspect ratios less than 10^{-6} and prolate spheroid rods of aspect ratios of less than 10^{-3}. Ferromagnetic conductors that retain a high permeability, of the order of 10^{6} (Gauss units) over the frequency bands of interest would comprise the most efficient

materials. Non-magnetic conductors such as aluminum, with conductivities of 10^{17} sec $^{-1}$ densities of 2 gms/cc offer extreme efficiency in absorption with requirements of 10^{-3} gms per square meter for greater than 95% absorption.

The extreme aspect ratios requirements for disks and rods are reduced for metal layered spheroids of low permittivity low density material like polystyrene, while still maintaining a mass per unit area requirement that is comparable to the solid particle distribution.

Metallurgical science, motivated by a variety of industrial applications unrelated to electromagnetic absorption, has emphasized fine particle technology for more than two decades. Therefore established and referenced techniques exist for the metallic coating of ultrafine non-metallic particles, the production of non-spherical particles in the form of filaments or flakes, and, more recently, the manufacturing of metal fibers or whiskers with very high length to diameter ratios for diameters in the submicron region. Further particle preparation and dispersal technology is available from referenced developments in aerosol science applied to inhalation health studies, such as in the production of fiber sized particles, the acoustic agglomeration of aerosols, particle classification and dust generator dispersal techniques.

The dispersal kinetics of aerosol sized metal particles may be modeled in a direct manner as

- isothermal expansion of the particle sustaining gas in vacuum or near vacuum conditions
- adiabatic expansion of the sustaining gas in an ambient atmosphere.

In the isothermal case, simulating free expansion the inverse square particle

number density dependence permits a simple attenuation path integral formulation of the percentage power absorption and hence the effectiveness duration of an ejected uniform density pulse of absorbing particles. In the adiabatic, ambient atmosphere case, the concentration expands to a volume compatible with atmospheric pressure and remains confined undergoing a diffusion process. The aerosol depleting processes in this case are the Brownian type of diffusion of the particles beyond the equilibrium volume, and flow field velocities relative to the dispersing source.

First order experimental testing of the power absorption principles can be carried out in a simple and direct manner by conventional methods of R.F. measurement of the changes in the power reflected and transmitted by previously calibrated dielectric plates that have been loaded. The loadings consist of prescribed concentrations of the different classes of absorbing particles discussed - low aspect metal filaments, flakes, metal coated ultrafine dielectric particles of low permittivity.

The greatest initial expense will be incurred in the generation of properly loaded dielectric samples. With polystyrene or polyeurathane as the dielectric base for supporting the varieties of loadings a representative estimate offered by an organization that is established in radar material R&D and manufacturing is in the vicinity of $10,000 for the several plate recipes.

A typical experimental configuration entails transmission across and reflection within shielded enclosures for a discrete set of frequencies. Apart from dielectric loading, the costs expected in the experimental testing will average $700 a day, for about a week of testing, or alternatively, about

$100 per frequency per sample.

Similar smaller scale measurements can be carried out by broadband microwave network reflection and attenuation measurement systems.

RECOMMENDATIONS

- The feasibility of experimentally testing dielectrics loaded with efficient absorbers, solid metal or metal coated non-conductors was alluded to in the previous section. Such transmission or attenuation and reflection measurements on a limited scale are recommended as a first order test of the conclusion and to determine effective and realizable concentrations particle shape, and layer parameters.

- An important question, as yet unanswered is the lower limit of particle size for effectively low depolarization or the maintenance of high absorption to scattering cross section ratio; that is,sizes of dimensions that are less than the conduction electron mean free path, thus having a higher anomalous collision frequency. The ratio of metal particle thickness to length, or metal layer thickness to curvature radius for metal coated hyperfine dielectric granules, determines the efficiency in external field penetration, and hence efficiency in absorption by Ohmic heating, provided that the thickness is less than skin depth. The reason for this is that the depolarizing field, proportional to the average solid angle subtended by the induced surface charge, becomes negligible for thin particles or layers with the longer dimensions parallel to the incident electric vector. Thus the tangential field penetrates to its skin depth limit, and thicknesses greater than skin depth represent superfluous mass. Efficiency in absorption, in terms of absorbed power to mass ratio (or non-dimensionally - absorbed to scattered power ratio) for a given frequency, therefore requires thicknesses less than the corresponding skin depth. For application to increasingly higher frequencies, the particle size or thickness must diminish accordingly. Since the optimum polarizability

of a particle diminishes with frequency increase, as the conductivity to frequency ratio, it is evident that suitably thin dimensions become more essential. On the other hand, as particle thickness reduces, the conductivity decreases and becomes more anomalous due to wall surface enhancement of the electron collision frequency. Thus a particle size limit may exist where the trend towards mass reduction efficiency is counteracted or significantly modified by reduction in conductivity. (More basic, but for much smaller distance scales is the quantum mechanical size limit below which the free conduction electron model no longer applies, for small agglomerations of atoms in which edge or boundary effects significantly distort the lattice electron conduction bands.)

It is recommended that a study be carried out to investigate the transition to anomalous conductivity or anomalous skin effect as the particle thickness reduces to dimensions below its bulk electron mean free path value. The study should consider thin metal film conduction and extension to thin wire filaments. The objective in mind is the functional behavior of the particle polarizability, the ratio of conductivity - volume fraction product to frequency, hence proportional to the product of conductivity and the skin depth.

- Another topic of importance is a more complete understanding of the function and capabilities of ferromagnetic effects in modifying RF absorption, in the present context of distributions of small ferromagnetic conducting particles or layers. It is the case that permeabilities of ferromagnetic materials can be considerably enhanced when they are in the form of fine particles, of micron or less dimensions comparable to the size of magnetic domains. At the same time the resultant permeability in a

microwave field undergoes nonlinear modification, possibly due to induced eddy currents, and may be substantially reduced from its D.C. value. The competing effects of D.C. permeability enhancement due to fine particle decomposition, into domain sizes, and A.C. degradation of the resultant permeability should be investigated in the context of dilute distributions. The impact of these tradeoffs on the composite medium permeability for weak fields should be explored inasmuch as the extinction depth is inversely proportional to it. Hence a significantly high retention of ferromagnetic permeability in the composite dielectric distribution would signify a correspondingly high improvement in power absorption to mass.

- The high absorption capabilities of more naturally occuring small, highly irregularly shaped metal particles have been noted, and merit further study. Such properties of simple spheroidal-like convex surfaces have been accessible to direct analysis in the Rayleigh limit for submicron dimensions. However, the analysis of irregular surfaces is more complex and less well defined. Irregularly shaped conducting particles are the most abundant in natural form, or resulting from imperfect production methods. A Rayleigh size conducting particle with a high degree of surface irregularity may be considered a superposition of sharply edged filaments or flakes. Hence its effective depolarizing factor may average out to a very small value, the small average value of the solid angle subtended by components of its surface normal to incident electric field vector. An approach to the study of irregular particle absorption in the Rayleigh submicron region would consider a statistical irregular surface formulation coupled with the solid angle interpretation of the depolarizing factor.

REFERENCES AND BIBLIOGRAPHY

1. M. Born, and E. Wolf, Principles of Optics, Chapt. 13, Pergamon Press, New York, 1959.

2. Jackson, J., Classical Electrodynamics, Sect. 4.6. Wiley, New York, 1962.

3. Reference 1, Section 2.4.

4. Reference 2, Section 9.6.

5. Stratton, and L. Chu, Phys. Rev. 56, 99, 1939.

6. Silver, S., Microwave Antenna Theory and Design, Rad. Lab Series 12, Sections 3.8 - 3.11. McGraw-Hill, New York, 1949.

7. Kleinman, R., Low Frequency Electromagnetic Scattering, Electro magnetic Scattering, P. Uslenghi, Ed., Academic Press, New York, 1980.

8. Greenberg, M., Focussing in on Particle Shape, Light Scattering by Irregularly Shaped Particles, D. Scheuerman, Ed., Plenum Press, New York, 1980.

9. Kerker, M., Scattering of Light and other electromagnetic radiation, Chapt. 10, Academic Press, New York, 1969.

10. Swinford, H., Electromagnetic Behavior of Radar Absorbing Chaff (RAC), Technical Note 354-43, June 1975 Naval Weapons Center, China Lake, California 93555.

11. Reference 9, Section 9.4.3.

12. Wilson, A., Theory of Metals, Chapt. 8, Cambridge, New York, 1965.

13. Ginzburg, V., Propagation of Electromagnetic Waves in Plasma, Chapt. 8 Pergamon, New York, 1978.

14. Loftman, K. A., Coatings Incorporating Ultra Fine Particles, Ultra Fine Particles, Eds. Kuhn, Lamprey and Sheer, Wiley, New York, 1963.

15. Van de Hulst, H., Light Scattering by Small Particles, Chapt. 19, Wiley, New York, 1957.

16. Reference 1, Section 13.5.

17. Swinford, H. and W. Cartwright, A Short Derivation of the Absorptive Scattering Properties of Short Filamentary Chaff, N.W. C Technical Memorandum 3718, March 1979, Naval Weapons Center, China Lake, California, 93555.

18. Luoma, E, ECCO Reflector Brochure, Emerson and Cuming, Inc., Canton, Mass., 1976.

19. Bozorth, R., Ferromagnetism, Chapts. 17, 18 Van Nostrand, New York, 1951.

20. Kittel, C., Theory of Structure of Ferromagnetic Domains, Phys. Rev. 70, 965-71.

21. B. Meddings, W. Kunda, and V. Makiw, Preparation of Nickel Coated Powders , in Powder Metallurgy , W. Leszinski Editor, Interscience, New York, 1960

22. R. Dixon and A. Clayton, Powder Metallurgy for Engineers , Machinery Publishing Co. Ltd., 1971 (England).

23. Backensto, A., Commercial Methods for Powder Production , in Vol. 3. Iron Powder Metallurgy , Editors Hausner, Rolland, Johnson, Plenum Press, New York, 1968.

24. Spurny, K., Fiber Generation and Length Classification ,in Reference 6.

25. Generation of Aerosols and Facilities for Exposure Experiments , K. Willecke, Editor, Ann Arbor Science, Ann Arbor, Mich., 1980.

26. Shaw, D., Acoustic Agglomeration of Aerosols in Reference 25.

27. Piatti, G., Preparation of New Multi-Phase Components , in Proceedings of the International School of Physics , Enrico Fermi, Course LXI, Edited by G. Caglotti, North Holland, 1978.

28. K. Willecke and R. Pavlik, Opposing Jet Classification , in Reference 25.

29. V. Marple and K. Rubow, -- Concepts and Parameters, in Reference 25.

30. N. Fuchs, and A. Sutugin, Highly Dispersed Aerosols, Chapt. 9, Ann Arbor Science Publishers, Ann Arbor, Mich., 1970.

31. Brock, J. The Kinetics of Ultrafine Particles, Aerosol Microphysics I, Particle Interaction, Ed. W. H. Marlow, Springer Verlag, New York, 1980.

32. Parker, W. H., Genistron RFI/EMI Analysis and Measurement Capabilities, Genisco Technology Corp., Rancho Dominguez, Ca. 90211, 1981.

33. Lance, A., Introduction to Microwave Theory and Measurement Systems, McGraw Hill, New York, 1964.

APPENDIX A
INTERNAL $\underline{E}$ FIELD CONSIDERATIONS

1. Integral Equation Formulation

The electric vector wave equation

$$\left(\nabla^2 + \frac{\omega^2}{c^2}\mu\right)\underline{E} = -4\pi\,\underline{\nabla}\rho - i\frac{\omega}{c}\left(\nabla\mu \times \underline{H}\right) - \frac{4\pi i\omega}{c^2}\mu\,\underline{j} \qquad (A1)$$

with Maxwell's equations and the vector Green's theorem, the Stratton-Chu integral formulation leads to the integral equation

$$\underline{E} = -\int d\underline{r}'\left\{\frac{i\omega}{c^2}\mu\,\underline{j}\,\Psi - \rho\underline{\nabla}\Psi\right\} + \underline{E}_0 \qquad (A2)$$

where the integral is over the volume of a particle with current and charge density $\underline{j}$ and ρ respectively. The far zone solution is obtained by setting

$$|\underline{r}| \simeq \underline{R} - \delta\underline{R}\cdot\underline{R}_1 \qquad \underline{R}_1 = |\underline{R}|^{-1}\underline{R} \qquad (A3)$$

changing integration variable from $\underline{r}$ to $\delta\underline{R}$, and integrating the transverse component of

$$\underline{E}_{far} = \frac{i\omega\mu}{c^2}\Psi(R)\int d\delta\underline{R}\left(\underline{j} - \underline{j}\cdot\underline{R}_1\right)e^{-ik_0\delta\underline{R}\cdot\underline{R}_1} + \underline{E}_0 \qquad (A4)$$

$$\underline{j} = \sigma\,\underline{E}_p$$

The current density $\underline{j}$ is thus determined from the solution to the interior equation (2) where only induced surface charge is assumed.

$$\rho = \underline{\nabla}\cdot\underline{E} = -\frac{\underline{\nabla}\cdot\underline{j}}{i\omega}\begin{cases} = 0 & \text{interior} \\ \simeq \rho_s & \text{surface charge density} \end{cases} \qquad (A5)$$

$$\rho = \rho_s\,\delta(|\underline{r} - \underline{r}_s|) = \rho_s\,\delta(r - r_s) \qquad \text{polar coordinates} \qquad (A6)$$

$$\rho_s = E_{n-} - E_{n+} = \left(1 - \frac{\varepsilon_1}{\varepsilon_0}\right)E_{n-}$$

across the surface by Gauss' Theorem.

Thus the internal field integral equation takes the form

$$\underline{E}_p = -\frac{i\omega}{c^2}\int d\underline{r}'\mu\sigma\underline{E}_p'\Psi(R') - \frac{1}{4\pi}\int ds'\frac{\Delta k}{k_0}(\underline{E}_p\cdot\underline{n})\underline{\nabla}\Psi + \underline{E}_0$$

$$\frac{\Delta k}{k_0} = \frac{k_1}{k_0} - 1 = \frac{4\pi\sigma}{i\omega} \qquad \text{(A7)}$$

Assume that the direction of $\underline{E}_p$ coincides with that of the incident field $\underline{E}_0$, polarized along the z axes and project (A7) in the $\underline{e}_z$ direction

$$E_p(\underline{r}) = -\frac{i\omega}{c^2}\int d\underline{r}'\mu\sigma E_p(\underline{r}')\Psi(R') + \frac{1}{4\pi}\int ds\,\frac{\Delta k}{k_0}\,\underline{e}_z\cdot\underline{n}\,E_p(\underline{r}_s')\partial_z\Psi(R') \qquad \text{(A8)}$$

$$+ E_0$$

Or since μ, σ are constant within the particle volume,

$$\underline{E}_p = -\frac{i\omega\mu\sigma}{c^2}\int d\underline{r}'E_p\Psi + \frac{i\sigma}{\omega}\int ds_z E_p\partial_z\Psi + E_0 \qquad \text{(A9)}$$

Eq (9) is the general form of the internal electric field equation for small particle size.

2. Ellipsoidal Scatterers

Here the vector equation (A7) is referred to

Let the ellipsoidal scatterer axes a_1, a_2, a_3, with directions $\underline{e}_1, \underline{e}_2, \underline{e}_3$, , . represent the reference coordinate system. Then

$$\underline{E}_p = \sum_{i=1}^{} (\underline{E}_p\cdot\underline{e}_i)\,\underline{e}_i = (E_1, E_2, E_3) \qquad \text{(A10)}$$

Then substitution of (A10) in (A7) results in the decomposition

$$E_k = -\frac{i\omega\mu\sigma}{c^2}\int d\underline{r}'E_k\Psi + \frac{i\sigma}{\omega}\int ds\,(\underline{e}_k\cdot\underline{n})E_k\frac{\partial\Psi}{\partial\rho_k}$$

$$+ \frac{i\sigma}{\omega}\int ds\sum_{i\neq k}'(\underline{e}_i\cdot\underline{n})E_i\frac{\partial\Psi}{\partial\rho_k} + E_{0k} \qquad \text{(A11)}$$

3. Rayleigh Size Particles

Now the Rayleigh condition is incorporated.

$$\max R \ll \lambda_0/2\pi \tag{A12}$$

where the maximum is taken over the particle volume. Condition (A12) then signifies that

$$\psi = \frac{e^{ik_0 R}}{R} \simeq \frac{1}{R} \tag{A13}$$

throughout the vector and scalar integrals depicting the internal field.

4. Constant Surface Value of E_p

The Helmholtz equation is separable in ellipsoidal coordinates. For sufficiently small dimensions the wave equation solutions are functions of only one "radial" variable which is constant on an ellipsoidal surface about the particle C.S. origin. If the Rayleigh conditions (A12) is assumed, as well as the constancy of the electric field magnitude on the inner surface, simplifications will arise which will then lead to self-consistent requirements on particle and field parameters. Thus assume

$$E_p(r_s) \simeq \text{const.} \tag{A14}$$

Then it follows that the second surface integral in (A11), containing the sum-exclusive of the k term - entails the closed line integral of exact differentials. Hence it is zero. Thus the projection of the internal field along the ellipsoidal axes in (A11) reduces to

$$E_k \simeq -\frac{i\omega\mu\sigma}{c^2}\int_{\delta V} d\underline{r}' E_k \psi(R) + \frac{i}{\omega}\sigma\int_S dS_k E_k \partial_{g_k}\psi + E_{0k} \tag{A15}$$

$$E_k \simeq \left[1 + \frac{i\sigma}{\omega} \left(\mu k_0^2 \int d\underline{r}' \frac{\epsilon(r')}{R'} - \int dS_k \frac{\partial}{\partial q_k} \left(\frac{1}{R} \right) \right) \right]^{-1} \cdot E_{0k} \qquad \text{(A16)}$$

Since $k_0 R \ll 1$, and $E_k(r_s) \simeq$ const.

($\epsilon(r)$ is a quantity of magnitude less 1).

Equation (A16) is an approximation that must be quantified.

The second term in the denominator,

$\mu k_0^2 \int_{av} d\underline{r} \frac{\epsilon}{R}$, is a constant with $\epsilon = 1$, for a sphere.

In terms of an effective penetration depth ,

$$\mu k_0^2 \int_{R \le \hat{R}} d\underline{r} \frac{\epsilon}{R} \le \mu k_0^2 \frac{8\pi}{3} \hat{R} \delta r \qquad \text{(A-17)}$$

for an ellipsoidal surface it is bounded as

$$\mu k_0^2 \int d\underline{r} \frac{\epsilon}{R} \le \mu k_0^2 2\pi \hat{R} \delta r_i \qquad \text{disk (oblate Spheroid)} \qquad \text{(A18)}$$

$$\le \mu k_0^2 3\pi \hat{\rho}^2 \delta r_r \qquad \text{rod (prolate Spheroid)} \qquad \text{(A19)}$$

where $\hat{R}, \hat{\rho}$ = larger Semi Axis for disk and rod, respectively.

5. Depolarizing Factor

The third term in the denominator of (A16) has the factor

$$\int dS_k \partial_{q_k} \left(\frac{1}{R} \right) = \int dS \frac{\partial}{\partial q_k} \left(\frac{1}{R} \right) \equiv P_e(k) \qquad \text{(A20)}$$

For ellipsoids, changing to ellipsoidal coordinates can express it as the constant ...

$$P_e(k) = 2\pi \int_0^\infty ds \frac{a_1 a_2 a_3}{(s+a_k^2)^{\frac{3}{2}} (s+a_j^2)^{\frac{1}{2}} (s+a_i^2)^{\frac{1}{2}}} \qquad \text{(A21)}$$

$P_e(k)$ is the depolarizing factor for axis k. As shown in (A20) it represents the average solid angle subtended by the induced surface charge.

For a sphere $$P_e(k) = P_e = 4\pi/3 \tag{A22}$$

When the ellipsoid scatterer is a spheroid, P_e has a closed form, with a, the longer axis, e_s the eccentricity,

$$e_s = \left(\frac{a_1^2 - a_2^2}{a_1^2}\right)^{\frac{1}{2}} \tag{A23}$$

when $a_1 = a_2 > a_3$, oblate or flattened spheroid

$$P_e'(3) = \frac{4\pi}{e_s^2}\left(1 - \left(\frac{1-e_s^2}{e_s^2}\right)^{\frac{1}{2}} \sin^{-1} e_s\right) \tag{A24}$$

for $a_1 = a_2 > a_3$, prolate or elongated spheroid

$$P_e'(1) = \frac{4\pi}{e_s^2}(1-e_s^2)\left[\frac{1}{2e_s} \ln\left(\frac{1+e_s}{1-e_s}\right) - 1\right] \tag{A25}$$

(Note (A24) and (A25) given by Reference 9

For the two equal axes

$$P_e' = (4\pi - P_e')/2 \tag{A26}$$

Thus for a circular disk,

$$P_e'(3) = 4\pi P_e'' = 0 \tag{A27}$$

while for the elongated spheroid

$$P_e'(1) = 0 \;, P_e'' = 2\pi \tag{A28}$$

Thus components of the internal field approximate to

$$E_p(k) = \frac{E_{0k}}{\left[1 - i\frac{\sigma}{\omega}(P_e(k) - \hat{\epsilon})\right]} \tag{A29}$$

$$\hat{\epsilon} = \mu k_0^2 \int d\tau \frac{\epsilon}{R} \tag{A30}$$

6. Applicability of Approximation

Equation (A29) is a meaningful approximation to the surface value of the internal field equation (A15) under two possible conditions

$$a)\quad P_e(k) >> \hat{\epsilon} \quad , \qquad b)\quad \left| P_e(k) - \hat{\epsilon} \right| < \frac{\omega}{\sigma} \tag{A31}$$

(A31) a is satisfied when

$$P_e(k) >> \frac{2\pi\mu\,\delta r_d}{\lambda_0} > \mu k_0^2\, 2\pi \hat{R}\, \delta r_d \tag{A32}$$

b)

$$P_e(k) >> 12\pi^3 \mu \frac{\hat{\rho}^2}{\lambda_0^2 L}\delta r_v > \mu k_0^2 \frac{3\pi\hat{\rho}^2}{L}\delta r_v \tag{A33}$$

while for a sphere

$$P_e(k) = \frac{4\pi}{3} >> \frac{16\pi^2\mu}{3\lambda_0}\delta r_s > \mu k_0^2 \frac{\rho}{3}\pi \hat{R}\, \delta r_s \tag{A34}$$

In the above, reference has been made to inequalities (A18) (A19) and (A17) respectively. When (A31)a is satisfied, equation (A29) (and hence (A16)) is consistently a statement about $E_k(s)$, the surface value of the internal field; the spatially depending term is negligible. Thus $\hat{\epsilon}$ can be discarded with small error and (A29) takes the form

$$E_k(s) \approx \frac{E_{0K}}{\left(1 - \frac{i\sigma}{\omega} P_e(k)\right)} \tag{A35}$$

When (A31a) obtains and for some $K = 1, 2$ or 3

$$P_e(k) >> \frac{\omega}{\sigma} \tag{A36}$$

The internal field for that component K is significantly depolarized

$$E_R \approx i\frac{\omega}{\sigma}\frac{E_{oR}}{\rho_e} \qquad \text{(A37)}$$

$$|E_R| \angle\angle |E_{oR}|$$

When (31b) applies, the depolarizing field is negligible. In this case inequalities for sufficiency in (31b) are

max $$\max\left(\rho_e(\kappa), \max\hat{\epsilon}\right) \angle\angle \frac{\omega}{\sigma} \qquad \text{(A38)}$$

$$\max \epsilon = \mu k_o^2 2\pi R \delta r_d \qquad \text{disk(A39)}$$

$$= \mu k_o^2 3\pi \rho^{*2} \delta r_r \qquad \text{rod (A40)}$$

The Sphere, because of its irreducible depolarization factor, and the extremely low numerical values of $\omega/\sigma \sim 10^{-7}$, cannot fulfill the above inequality (A38).

7. Matching Interior Wave Equation Solution to Boundary Value Integral

The Helmholtz equation within the particle is of the form

$$(\nabla^2 + k^2)\underline{E} = \left((\nabla^2 + k_o^2) + (k^2 - k_o^2)\right)\underline{E} = 0 \qquad \text{(A41)}$$

on multiplying by $\Psi/4\pi$ and integrating over the particle Volume

$$\int d\underline{r}\,\frac{\Psi}{4\pi}(\nabla^2 + k^2)\underline{E} + (k^2 - k_o^2)\int d\underline{r}\,\frac{\Psi}{4\pi}\underline{E} = 0 \qquad \text{(A42)}$$

Now $\frac{\Psi}{4\pi} = \frac{e^{ik_o|\underline{r}-\underline{r}'|}}{4\pi|\underline{r}-\underline{r}'|}$ is the free space Green's function.

Thus on applying Green's theorem to (A42)

$$\int dS\left(\frac{\Psi}{4\pi}\partial_n\underline{E} - \frac{\partial_n\Psi}{4\pi}\underline{E}\right) + \underline{E} + (k^2 - k_o^2)\int d\underline{r}\,\frac{\Psi}{4\pi}\underline{E} = 0 \qquad \text{(A43)}$$

Thus

$$\int d\underline{r}\,\Psi E = \frac{1}{(k^2 - k_o^2)}\int dS\left(\partial_n\Psi\underline{E} - \Psi\partial_n\underline{E}\right) - \frac{4\pi\underline{E}}{(k^2 - k_o^2)} \qquad \text{(A44)}$$

Substitution of (A44) into (A9) reduces the integral equation to

$$0 = -\frac{1}{4\pi}\int dS\left(\partial_n \Psi E - \Psi \partial_n E\right) + \frac{i\sigma}{\omega}\int dS_2\, E\,\partial_2 \Psi + E_0 \tag{A45}$$

a form which requires only the surface values of $\underline{E}$ and its normal derivative.

Because $\nabla\cdot\underline{E}$ was set to zero in the interior, Equation (A9), as well as (A45) is not exact, there is a small volume integral term which is negligibly small in the Rayleigh limit.

Now if $\underline{E}$ is a function of the radial coordinate only, again for very small particle dimension to wave length ratio, E and $\partial_n E$ are constant in the surface. Thus set

$$E = C\,\mathcal{E}(\xi) \tag{A46}$$

for ξ the radial coordinate, and $\mathcal{E}$ the solution that is unity at the origin of the particle ellipsoid coordinate system.

The constant C is determined from Equation (A45).

$$C = \left\{\left(1 + \frac{i\sigma}{\omega} P_e\right)\mathcal{E}(\xi_s) - \left(\int dS\,\frac{1}{R}\right)\left(\partial_\xi \mathcal{E}\right)_{\xi_s}\right\}^{-1} E_0 \tag{A47}$$

The term $\int dS\,\frac{1}{R}$ integrated over the ellipsoidal surface is a constant since it refers to the potential at the interior of a surface of constant surface charge density, hence an equipotential surface. With (A47) the internal field (A46) then become

$$E(\underline{r}) = \frac{\mathcal{E}(\xi)\,E_0}{\left(1 + \frac{i\sigma}{\omega} P_e\right)\mathcal{E}_s - \phi_s\,\partial_n \mathcal{E}_s}$$

where

$$\mathcal{E}_s = \mathcal{E}(\xi_s),\quad \partial_n \mathcal{E}_s = \left(\partial_\xi \mathcal{E}(\xi)\right)_{\xi_s},\quad \phi_s = \int dS\,\frac{1}{R} \tag{A48}$$

8. Properties of the Radial Coordinate Solution

The function $\mathcal{E}(\xi)$ is typified by the three spheroidal limiting shapes, sphere, disk and rod

TABLE A-1 FUNCTIONAL FORMS OF RADIALLY DEPENDENT SOLUTION

Property / Shape	Limiting Radial coordinate	Internal Field Form
Sphere	Radius r	$C(\sin kr)/r$
oblate Spheroid Disk	Thickness x	$C' e^{ikr}$
Prolate Spheroid Rod	Thickness Radius ρ	$C'' J_0(k\rho)$ zero order Bessel function

for k = effective propagation vector magnitude in particle.

The spatial behavior of radial coordinate solution thus indicates that the internal field in (A48) achieves its maximum amplitude on the boundary surface S, then decays with a skin depth attenuation thickness k^{-1}. Inspection of (A48) also establishes that for larger depolarizing factors P_e, namely

$$P_e > \frac{\omega}{\sigma} \text{ , where,}$$

$$\underline{E}(\underline{r}) = \frac{-i\omega}{\sigma P_e} \frac{\underline{\mathcal{E}}(\xi)}{\mathcal{E}(\xi_s)} \underline{E}_0 \qquad \text{(A49)}$$

$$|\underline{E}(\underline{r})| \leq |\underline{E}(\underline{r}_s)| = \frac{\omega}{\sigma P_e} |\underline{E}_0|$$

Thus the (inner) boundary field is depolarized. The depolarization is negligible for

$$\underline{E}(\underline{r}) = \frac{\underline{\mathcal{E}}(\xi)}{\mathcal{E}(\xi_s)} \underline{E}_0 \quad , \quad |\underline{E}(\underline{r})| < E(r_s) = E_0 \qquad \text{(A50)}$$

9. Penetration Depth Identified

The penetration depths δr_s, δr_d, δr_t used in Equations (A17), (A18), (A19), (A32), (A34), (A39) and (A40). Thus refer to a dimension of less than the skin depth of the solid metal particle.

$$d \leq \delta r_{sk} = \frac{c}{2\pi} \frac{1}{\sqrt{2\sigma\mu f}}$$

10. Conducting Shell

The particle size condition remains fulfilling the Rayleigh Scattering criterion. Namely the largest linear dimension $\hat{R}$ must be such that $\hat{R} \ll \frac{\lambda_0}{2\pi}$, for λ_0 the free space wavelength, or $k_0 \hat{R} \ll 1$, the free space wave number. Another distance scale associated with scattering from Rayleigh size, conducting particles is the effective penetration depth d. As indicated in the previous section this depth d is bounded by the skin depth

$$d \leq \delta r_{sk}$$

Now consider a thin shell, in the shape of a spheroid, which may be hollow or filled with a weak dielectric that is transparent to the incident RF or microwave radiation. The spheroid shape also fulfills the Rayleigh condition, and its orientation with major axis parallel to the incident electric vector offers a minimal "depolarizing" factor $P_e(1)$. The Stratton-Chu based integral equation for the field internal to the spheroid shell would be similar to that of the solid spheroid conductor, however, the principal change would be in the effective depolarizing factor of the shell.

Equation (A45) when referred to shell geometry becomes

$$0 = \frac{-1}{4\pi} \int dS \left(\partial_n \psi \cdot E - \psi \partial_n E\right) + i\frac{\sigma}{\omega} \int dS_2 E \partial_2 \psi + E_0$$

$$= \frac{-1}{4\pi} \left\{ \int_S - \int_{S-\delta S} \right\} dS \left(\partial_n \psi E - \psi \partial_n E\right) + \frac{i\sigma}{\omega} \left\{ \int_S - \int_{S-\delta S} \right\} dS_2 E \partial_2 \psi + E_0 \quad (51)$$

a) if the thickness of δS is greater than skin depth δr_{sk}, all the surface integrals over $S-\delta S$ are negligible, approximate to zero, and the shell solution is the same as the solid (but with reduced mass).

b) if the thickness is less than δr_{sk}, the surface value of the field E is constant and (A51) becomes

$$0 = -E_s\left\{\int_S - \int_{S-\delta s}\right\} ds\, \frac{\partial_n \psi}{4\pi} + \partial_n E_s \left\{\int_S - \int_{S-\delta_s}\right\} ds\, \frac{\psi}{4\pi}$$

$$+ \frac{i\sigma}{\omega} E_s \left\{\int_S - \int_{S-\delta_s}\right\} dS_2\, \partial_2 \psi + E_0 \qquad \text{(A52)}$$

$$0 = E_s - \partial_n E_s\, \delta\left(\int_s ds\, \psi\right) + \frac{i\sigma}{\omega} E_s\, \delta(P_e) \qquad \text{(A53)}$$

where the variation is taken with respect to the layer thickness, in the direction of the surface normal.

Thus

$$\delta\left(\int_s ds\,\psi\right) = \delta r_s \frac{\partial}{\partial r_s}\left(\int d\Omega \frac{r_s^2}{|\vec{r}-\vec{r}_s|}\right)$$

$$= 2\int d\Omega \frac{r_s^2}{|\vec{r}-\vec{r}_s|}\left(\frac{\delta r_s}{r_s}\right) - \delta r_s \int ds\, \partial_n\left(\frac{1}{|\vec{r}-\vec{r}_s|}\right)$$

$$\delta\left(\int_s ds\,\psi\right) = 2\int ds\,\psi \frac{\delta r_s}{r_s} - 4\pi\,\delta r_s$$

while the more important term ....

$$\delta P_e = \delta r_s \frac{\partial}{\partial r_s}\int d\Omega\, r_s^2 \cos\phi\, \partial_2\left(\frac{1}{|\vec{r}-\vec{r}_s|}\right) = \delta r_s \frac{\partial}{\partial r_s} P_e \qquad \text{(A54)}$$

$$= 2\int d\Omega \left(r_s^2 \cos\phi\, \partial_2 \frac{1}{|\vec{r}-\vec{r}_s|}\right)\left(\frac{\delta r_s}{r_s}\right) - \int ds \cos\phi \frac{\partial}{\partial r_s}\partial_2 \frac{1}{|\vec{r}-\vec{r}_s|} \qquad \text{(A55)}$$

For a sphere $\frac{\partial}{\partial r_s} = -\frac{\partial}{\partial r}$ in the second term on the right in (A55), which in turn indicates that the value of that term is zero. Thus

$$\delta P_e = 2 \frac{\delta r_s}{r_s} P_e = \frac{8\pi}{3} \frac{\delta r_s}{r_s} \qquad \text{(A56)}$$

(sphere)

Similarly for general spheroids the derivative of the solid's depolarizing factor applies, as in (A54). The result for the sphere can also be obtained from the spheroid in the limit as the eccentricity goes to zero.

The general form of the depolarizing factor for a thin shell can be determined by differentiation of the expressions in (A24), A25), (A26) with the eccentricity ϵ_s defined in (A23).

However for larger eccentricities the results simplify to

oblate spheroid shell disk $\delta P_e \simeq P_e \cdot \frac{\delta r_s}{a \text{ (minor)}}$ (A57)

prolate spheroid shell rod $\delta P_e \simeq 2P_e \cdot \frac{\delta r_s}{a \text{ (minor)}}$ (A58)

for $\frac{a \text{ (minor)}}{a \text{ (major)}} < 1$. (A59)

11. Summary, Limiting Depolarizing Factors

The following Table A-2 is a summary

TABLE A-2 LIMITING DEPOLARIZING FACTOR OF SOME SHELL SHAPES

Shell Shape	P_e (solid)	(layer) δP_e
Sphere	$4\pi/3$	$(8\pi/3)(\delta r_s/r_s)$
disk	$\pi^2 (a_2/a_1)$	$\pi^2 \delta r_s/a_1$
rod	$(2\pi \ell n 2)(a_2/a_1)^2$	$(2\pi \ell n 2)(a_2/a_1)(\delta r_s/a_1)$

a_2 = minor axis, a_1 = major axis, $a_2/a_1 << 1$

12. High Permeability Particle

Here, the μ of the particle may be greater than 1. The electric field equation (A41) takes the form

$$\left(\nabla^2 + \frac{\omega^2}{c^2}\right)\underline{E} = \frac{\omega^2}{c^2}(1-\mu)\underline{E} + \frac{4\pi i}{c^2}\omega\,\underline{j} \qquad \text{(A60)}$$

on applying the free space Green's function with the condition that the particle size fulfills the free space Rayleigh criterion, radius rs,

$r_s < \lambda_0/2\pi$, (but not necessarily modified Rayleigh).

$$\underline{E} = \int d\underline{r}' \left\{ \frac{e^{ik_0 R}}{R}\left(\frac{\omega^2}{c^2}(1-\mu) + i\frac{\omega\mu\sigma}{c^2}\right)\underline{E}(\underline{r}') + \frac{\sigma}{i\omega}\underline{\nabla}\cdot\underline{E}\;\underline{\nabla}\frac{e^{ik_0 R}}{R}\right\} + \frac{i\sigma}{\omega}\int dS\,(\underline{E}\cdot\underline{n})\,\underline{\nabla}\frac{e^{ik_0 R}}{R} \qquad \text{(A61)}$$

on assuming that the field E is substantially constant from the surface r_s down to $r_s - \delta r_s$, $r_s <$ skin depth δr_{s_a} ,

$$E \simeq \left\{ 1 + \int_{V(r_s - \delta r_s)}^{V(r_s)} d\underline{r}\,\frac{1}{|\underline{r} - \underline{r}_s|}\left(\frac{\omega^2(1-\mu)}{4\pi c^2} - i\frac{\omega\mu\sigma}{c^2}\right) + \frac{i\sigma}{\omega}\int_{S-\delta S}^{S} dS_2\,\partial_2\left(\frac{1}{R}\right)\right\}^{-1} \cdot E_0 \qquad \text{(A62)}$$

or for a sphere

$$E = \left\{ 1 + 4\pi r \delta r \left(\frac{\omega^2 (\mu - 1)}{4\pi c^2} - i \frac{\omega \mu \sigma}{c^2} \right) + i \frac{8\pi}{3} \frac{\sigma}{\omega} \frac{\delta r_s}{r_s} \right\}^{-1} E_0 \qquad \text{(A63)}$$

The requirement on E is that it be constant in layer δr_s

This is fulfilled if

$$\text{a)} \quad 1 > r \delta r k_0^2 (\mu - 1) \qquad \text{(A64)}$$

and

$$\text{b)} \quad \left| r \delta r k_0^2 \mu - \frac{2}{3} \frac{\delta r_s}{r_s} \right| < \frac{\omega}{4\pi\sigma} \qquad \left(\frac{\delta r}{r} < \frac{\delta r_s}{r_s} \right) \qquad \text{(A65)}$$

consider b) first, and let

$$r_s < \sqrt{\frac{2}{3\mu}}\, k_0^{-1} < \frac{1}{\sqrt{\mu}}\, k_0^{-1} = r_0 \qquad \text{(A66)}$$

This is the modified Rayleigh condition.

Then b) is fulfilled when

$$\frac{\delta r_s}{r_s} \leq \frac{2}{3} \frac{\omega}{4\pi\sigma} \left(\frac{1}{1 - \frac{3}{2} r_s^2 k_0^2 \mu} \right) \qquad \text{(A67)}$$

Let $$r_s = r_0 (1 - \zeta) \qquad \text{(A68)}$$

Then (A67) becomes

$$\frac{\delta r_s}{r_s} \leq \frac{\omega}{4\pi\sigma\, 3(2 - \zeta)} \qquad \text{(A69)}$$

Comparison of skin depth with bound (A67)

The skin depth for frequency ω, $\delta r_{s_\omega}(\omega)$ is

$$\delta r_{s_\omega}^2 = \frac{c^2}{4\pi^2 \mu \sigma f} = \frac{\omega}{2\pi\sigma} r_0^2 \qquad \text{(A70)}$$

ro defined in (A66)

On squaring (A69)

$$\delta r_s^2 < \frac{\omega^2}{16\pi^2}\frac{r_0^2}{\sigma^2}\frac{(1-\zeta)^2}{\zeta^2(2-\zeta)^2} = \frac{\omega}{2\pi\sigma}\left(\frac{1-\zeta}{\zeta(2-\zeta)}\right)^2 \delta r_{s_k}^2 \qquad \text{(A71)}$$

Then since

$$\delta r_s = r_{s_{max}} - r \quad < r_0 \zeta \qquad \text{(A72)}$$

with (A72) as the stronger condition, (A69) implies

$$\left(\frac{2-\zeta}{1-\zeta}\right)^2 \zeta^2 \leq \frac{\omega}{4\pi\sigma} \qquad \text{(A73)}$$

Thus if (A73) is fulfilled, it follows that

$$\left(\frac{1-\zeta}{\zeta(2-\zeta)}\right)^2 \geq \frac{4\pi\sigma}{\omega} \qquad \text{(A74)}$$

satisfies (A73) and substituting on (A71) establishes

$$\delta r_s \quad < \delta r_{s_k} \qquad \text{(A75)}$$

the requirement that for a modified Rayleigh sphere the layer thickness over which the field is constant is less than skin depth.

APPENDIX B

COMPOSITE PERMITTIVITY OF DISTRIBUTIONS

1. Particle Polarizability

The internal field component E_i drives the conduction electrons to give rise to the current density

$$\underline{J}_i = \sigma \underline{E}_i = i\omega \underline{P}_i \qquad \text{(B1)}$$

where

$\underline{P} = (P_1, P_2, P_3)$ Polarization per particle electric dipole moment/

Let $\underline{\mathcal{P}} \equiv$ total electric dipole moment/particle

$= \underline{P} \times$ volume of particle.

Then on using equations (A29), (A30) for E_i

$$\mathcal{P}_k = P_k \Delta V = \frac{1}{i\omega} J_k \Delta V = \frac{\sigma}{i\omega} \frac{E_{0k} \Delta V}{\left(1 + \frac{\Delta k}{4\pi k_0} P_{ek} + \hat{\epsilon}_k\right)} \qquad \text{(B2)}$$

$$\frac{\Delta k}{4\pi k_0} = \frac{\sigma}{i\omega}$$

Thus for a particle of polarizability $\underline{\alpha}$ where

$$\alpha_k = \frac{1}{4\pi} \frac{\Delta k}{k_0} \frac{1}{\left(1 + \frac{\Delta k}{4\pi k_0} P_{ek} + \hat{\epsilon}_k\right)} \qquad \text{(B3)}$$

electric dipole moment per unit particle volume per unit electric field

The total electric dipole moment

$$\underline{\mathcal{P}} = \sum_{k=1}^{3} \underline{e}_k \left(\underline{e}_k \cdot \underline{E}_0\right) \alpha_k \Delta V \qquad \text{(B4)}$$

Let the direction of the incident $\underline{E}$ vector be $\underline{e}_z$.

Then project $\underline{\mathcal{P}}$ on to $\underline{e}_z$ ... .

$$P_z = \sum_{k'=1}^{3} (\underline{e}_{k'} \cdot \underline{e}_z) E_{oz} \Delta V \tag{B5}$$

on averaging over the . . .

$$\langle P_z \rangle = \left(\frac{1}{3} \sum_{1}^{3} \alpha_{k'} \right) \Delta V \, E_{oz} \tag{B6}$$

= average z-component of dipole moment/particle.

2. Particle Number Density

Each particle has axes a_1, a_2, a_3, therefore one formulation of the particle number density is $\hat{m}(\underline{a})$ = number of particles/vol in $\underline{a} = (a_1, a_2, a_3)$ space

$$dN(a_1, a_2, a_3) = \hat{m}_a(\underline{a}) d\underline{a} = \bar{N} f_a(\underline{a}) d\underline{a} \tag{B7}$$

where $\bar{N}$ = mean number density.

Equivalently the number density can be defined over the depolarizing factor space $\underline{P}_e = (P_{e_1}, P_{e_2}, P_{e_3})$

$$dN(P_{e_1}, P_{e_2}, P_{e_3}) = \hat{m}_p(\underline{P}_e) d\underline{P}_e = \bar{N} f_p(\underline{P}_e) d\underline{P}_e \tag{B8}$$

3. Effective Field

For dilute distributions with uniformly distributed dipoles, the field at the center of any spherical surface is the average quantity

$$\underline{E}_{eff} = \bar{\underline{E}} + \frac{4\pi}{3} \bar{\underline{P}} \tag{B9}$$

$\bar{\underline{P}}$ = (average number of particles/vol) x (average dipole moment/particle)

$$\bar{\underline{P}} = \bar{N}_p \left(\int d\underline{a} \, \hat{f}_a(\underline{a}) \cdot \frac{1}{3} \sum_{1}^{3} \alpha_i \Delta V \right) E_{eff}$$

$$= \bar{N}_p \left(\int d\underline{P}_e \, \hat{f}_{P_e}(\underline{P}_e) \cdot \frac{1}{3} \sum_{1}^{3} \alpha_i \Delta V \right) E_{eff}$$

$$\bar{P} = \bar{N}\,\overline{\alpha\Delta V}\,E_{eff} \tag{B10}$$

Thus on using (B10) in (B9)

$$\underline{E}_{eff} = \frac{1}{\left(1 - \frac{4\pi}{3} N \overline{\alpha\Delta V}\right)}\,\overline{\underline{E}} \tag{B11}$$

4. Effective Permittivity

Then with the usual constitutive relation between electric displacement, electric field and polarization,

$$\underline{D} = \epsilon\,\underline{E} = \underline{E} + 4\pi\,\underline{P} \tag{B12}$$

The permittivity or dielectric constant becomes

$$\epsilon = \frac{1 + \frac{8\pi}{3}\bar{N}\,\overline{\alpha\Delta V}}{1 - \frac{4\pi}{3}\bar{N}\,\overline{\alpha\Delta V}} \tag{B13}$$

as the Clausius-Mosotti, Lorentz - Lorenz Law.

5. Strong and Weak Absorber Decomposition

The individual particle polarizability α_k, is given in (B3),

$$\alpha_k = \frac{i\sigma}{\omega}\,\frac{1}{\left(1 + i\frac{\sigma}{\omega}\underline{P}_{e\pi} + \hat{\epsilon}_k\right)} \tag{B14}$$

Let the fractional number density be decomposed into

$$f(\underline{P}_e) = f_1(\underline{P}_e) + f_2(\underline{P}_e) \tag{B15}$$

where 1 denotes particles with very small depolarizing factors

$$(\underline{P}_e)_1 = \delta_1 \leq \frac{\omega}{\sigma} \tag{B16}$$

and for particles with larger depolarizing factors

$$(\underline{P}_e)_2 > \frac{\omega}{\sigma} \tag{B17}$$

Then

$$\left(\frac{1}{3}\sum_{1}^{3}\alpha_k \Delta V\right)_1 \simeq \frac{1}{3}\,\frac{i\sigma}{\omega}\,\frac{\Delta V_1}{(1+i\bar{\delta}_1+\hat{\epsilon}_1)} \tag{B18}$$

$$\left(\frac{1}{3}\sum_{1}^{3}\alpha_k \Delta V\right)_2 \simeq \frac{1}{3}\left(\sum_{1}^{3}\frac{1}{P_{e_k}}\right)_2 \Delta V_2 \tag{B19}$$

Therefore the average polarizability of the distribution of particles, namely $\overline{N\alpha\Delta V}$ in Equation (B13), is expressed as

$$\bar{N}\,\overline{\alpha\Delta V} = \frac{1}{3}\,\frac{i\sigma}{\omega}\,\frac{F_1}{(1+i\bar{\delta}_1+\hat{\epsilon}_1)} + \left\langle\frac{1}{P_{e_2}}\right\rangle F_2 \tag{B20}$$

where

$F_1 = \overline{N\Delta V_1}$ = total average volume fraction of type 1 particles

$F_2 = \overline{N\Delta V_2}$ = total average volume fraction of type 2 particles

$\left\langle\frac{1}{P_{e_2}}\right\rangle$ = average reciprocal depolarizing factor of type 2 particles. (Because of the smallness of δ_1 and ϵ_1, they are replaceable by their averages.)

Thus the composite permittivity, equation (B13) takes the form

$$\epsilon = \frac{1+\frac{4\pi}{3}\left(\frac{i\sigma}{3\omega}F_1\frac{1}{(1+i\delta_1+\epsilon_1)}+\left\langle\frac{1}{P_{e_2}}\right\rangle F_2\right)}{1-\frac{4\pi}{3}\left(\frac{i\sigma}{3\omega}F_1\frac{1}{(1+i\delta_1+\epsilon_1)}+\left\langle\frac{1}{P_{e_2}}\right\rangle F_2\right)} \tag{B21}$$

Two limiting cases of (B21) are for

a) $F_1 \gg \frac{3\omega}{\sigma}\left\langle\frac{1}{P_{e_2}}\right\rangle F_2$ (B22)

giving rise to

$$\epsilon \approx \frac{1 + i\frac{8\pi\sigma}{9\omega}F_1}{1 - i\frac{4\pi}{9}\frac{\sigma}{\omega}F_1} + O\left(\frac{3\omega}{\sigma}\left\langle\frac{1}{\rho_{e_2}}\right\rangle F_1\right) \tag{B23}$$

b) $$F_1 << \frac{3\omega}{\sigma}\left\langle\frac{1}{\rho_{e_2}}\right\rangle F_2 \tag{B24}$$

where

$$\epsilon \approx \frac{1 + \frac{8\pi}{3}\left\langle\frac{1}{\rho_{e_2}}\right\rangle F_2}{1 - \frac{4\pi}{3}\left\langle\frac{1}{\rho_{e_2}}\right\rangle F_2} \tag{B25}$$

6. Refraction, Extinction, and Mass Requirements

For very dilute distributions fulfilling a) such that

$$\frac{3\omega}{\sigma} \geq F_1 \geq \frac{3\omega}{\sigma}\left\langle\frac{1}{\rho_{e_2}}\right\rangle F_2 \tag{B26}$$

The index of refraction is

$$n = \sqrt{\epsilon} \approx 1 + i\frac{2\pi}{3}\frac{\sigma}{\omega}F_1 \tag{B27}$$

with a field strength attenuation factor

$$\hat{a} = \frac{\omega}{c}\,\mathrm{Im}\sqrt{\epsilon} = \frac{2\pi}{3c}\sigma F_1$$

an extinction depth

$$\chi_d = \frac{1}{\hat{a}} = \frac{3c}{2\pi\sigma F_1} \tag{B28}$$

an extinction cross section , per unit particle Volume

$$\frac{\sigma_x}{\Delta v} = \frac{\hat{a}}{F_1} = \frac{2\pi}{3c}\sigma \tag{B29}$$

and the mass M, requirements for extinction across area A

$$M = A\chi_d\rho F_1 = \frac{3c}{2\pi\sigma}\rho A \qquad \text{gms}$$

ρ = density of metal (gms/cm^3) (B30)

7. Power Reflection, Absorption Coefficients

For general, dilute, distributions fulfilling condition A, the power reflection coefficient, R, at normal incidence for slab geometry as

$$R = \left| \frac{\sqrt{\epsilon} - 1}{\sqrt{\epsilon} + 1} \right|^2 \tag{B31}$$

for

$$\epsilon = \frac{1 + 2i\beta}{1 - 2i\beta} \quad , \quad \beta = \frac{4\pi}{9} \frac{\sigma}{\omega} F_1 \tag{B32}$$

R, the transmission coefficient A = 1-R, and the extinction depth x_d to incident wavelength ratio is

$$\frac{x_d}{\lambda} = \frac{1}{2\pi \, Im \sqrt{\epsilon}} \tag{B33}$$

R, A=1-R and $\frac{x_d}{\lambda}$ are plotted as functions of β in Figure (B-1)

8. Estimate of Low Depolarizing Factor Particle Size

Since Case a) assumes the concentrations of particles with low depolarizing factors predominate, the particle geometry for spheroids is to be specified

a) Oblate spheroid (disk), Equation (A24) and (A23) respectively are repeated

$$P_e'(3) = \frac{4\pi}{e_s^2} \left(1 - \left(\frac{1 - e_s^2}{e_s^2} \right)^{\frac{1}{2}} \sin^{-1} e_s \right) \tag{B34}$$

$$e_s = \left(1 - \frac{a_1^2}{a_2^2} \right)^{\frac{1}{2}} \qquad a_1 < a_2 = a_3 \tag{B35}$$

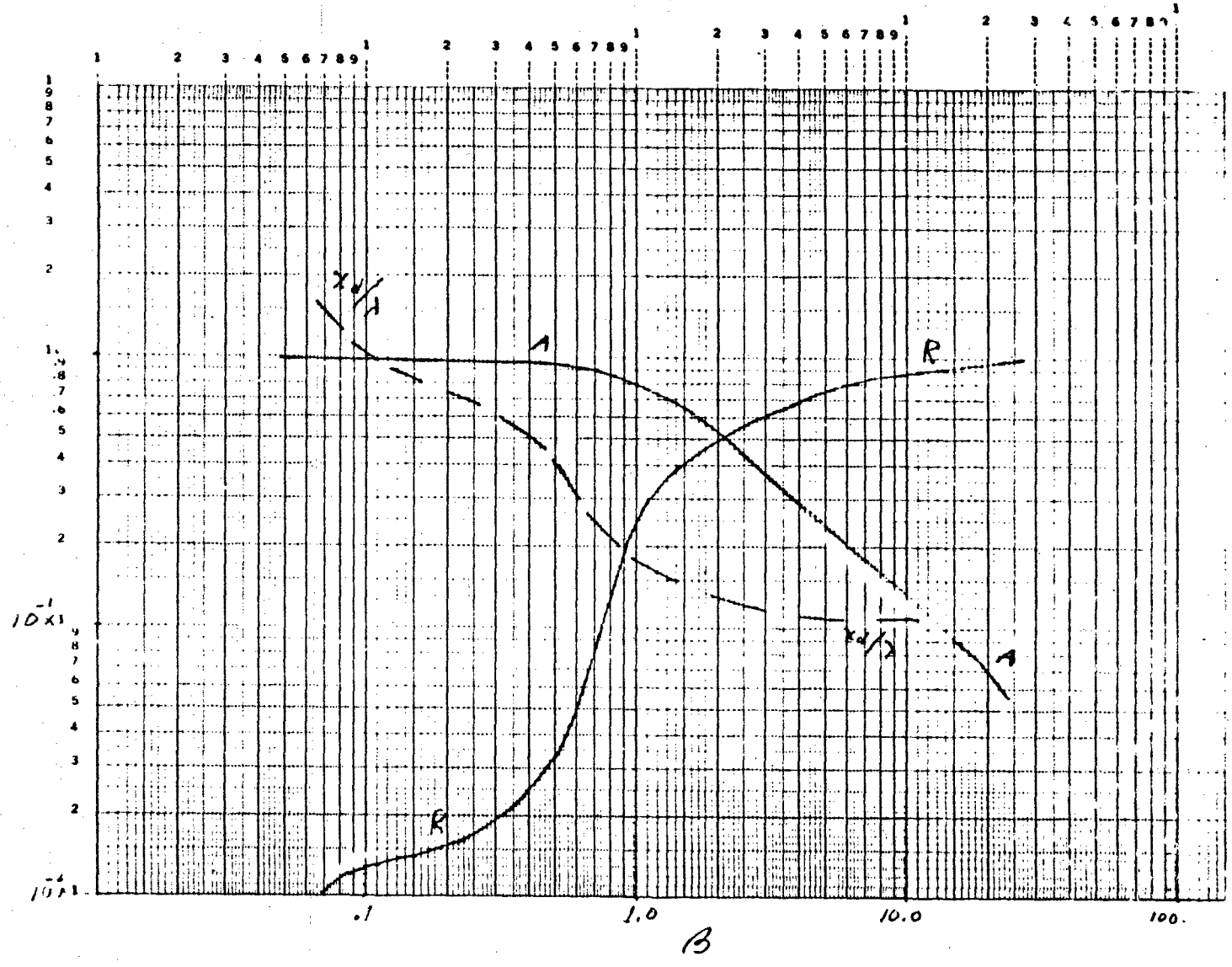

Figure B1.- Power Reflection/Absorption of Efficient Absorbers vs β

$$P_e'(3) \simeq 4\pi\left(1 - \frac{1}{2}e_c + e_c^{\frac{1}{2}}\frac{\pi}{2}\right), \quad e_c = 1 - e_s^2$$

$$P_e'' = 2\pi\left(1 - \frac{P_e'(3)}{4\pi}\right) \simeq \pi^2 \frac{a_2}{a_1} < \frac{\omega}{\sigma} = \frac{2\pi f}{\sigma}$$

Thus $\frac{a_2}{a_1} < \frac{2f}{\sigma}$ small depolarizing factor for disk (B37)

b) Prolate spheroid (rod) (A25)

$$P_e(1) = \frac{4\pi}{e_s^2}(1-e_s^2)\left(\frac{1}{2e_s}\ln\left(\frac{1+e_s}{1-e_s}\right) - 1\right), \quad a_1 > a_2 = a_3 \quad \text{(B38)}$$

let $e_c = \left(\frac{a_3}{a_1}\right)^2 = 1 - e_s^2$

Then

$$P_e(1) = 2\pi e_c \ln\left(\frac{1}{e_c}\right) < \frac{\omega}{\sigma} = \frac{2\pi f}{\sigma} \quad \text{(B39)}$$

$$e_c \ln\left(\frac{1}{e_c}\right) < \frac{f}{\sigma}$$

$$\frac{a_2}{a_1} < \left(\frac{\frac{f}{\sigma}}{\ln\left(\frac{\sigma}{f}\right) + \ln\left(\ln\frac{\sigma}{f}\right)}\right)^{\frac{1}{2}}$$

small depolarizing factor for rod (B40)

9. Single Species of Ellipsoids

a) Total Reflection, Slab Geometry

Here one axis $P_e(1) << P_e(2), P_e(3)$ (B41)

hence the spheroid is prolate, but not necessarily of minimal P_e fulfilling (B16). Thus the permittivity given by (B13), (B20), takes the form

$$\epsilon = \frac{1 + \frac{4\pi}{9} F \frac{i\sigma}{\omega} \frac{1}{\left(1 + i\frac{\sigma}{\omega} P_e(1) + \hat{\epsilon}\right)}}{1 - \frac{4\pi}{9} F \frac{i\sigma}{\omega} \frac{1}{\left(1 + i\frac{\sigma}{\omega} P_e(1) + \hat{\epsilon}\right)}} \quad \text{(B42)}$$

$$\epsilon = \frac{1 + \frac{4\pi}{9} F \left(P_e - i(1+\epsilon')\frac{\omega}{\sigma}\right)^{-1}}{1 - \frac{4\pi}{9} F \left(P_e - i(1+\epsilon')\frac{\omega}{\sigma}\right)^{-1}} \tag{B43}$$

Then if $$F >> \frac{9}{4\pi} P_e(1) > \frac{9}{4\pi} \frac{\omega}{\sigma} \tag{B44}$$

$$\epsilon \simeq -2 \;, \quad \sqrt{\epsilon} \simeq i\sqrt{2} \tag{B45}$$

and we have total reflection for normal incidence on a slab.

b) Dilute Distribution

Let $$\frac{4\pi F}{9\sqrt{P_e^2(1) + \frac{\omega^2}{\sigma^2}}} << 1 \qquad F << 9\sqrt{P_e^2(1) + \frac{\omega^2}{\sigma^2}} \tag{B46}$$

Then $$\epsilon \simeq 1 + \frac{4\pi}{3} F \frac{1}{\left(P_e(1) - i(1+\epsilon)\frac{\omega}{\sigma}\right)} \tag{B47}$$

$$\sqrt{\epsilon} = 1 + \frac{2\pi}{3} F \frac{1}{\left(P_e(1) - i(1+\epsilon')\frac{\omega}{\sigma}\right)} \tag{B48}$$

$$Im\sqrt{\epsilon} \simeq \frac{2\pi}{3} \frac{F\omega}{\sigma} \frac{1}{\left(P_e^2(1) + \frac{\omega^2}{\sigma^2}(1+\epsilon)^2\right)} \tag{B49}$$

extinction depth

$$\chi_d = \frac{3\sigma P_e^2(1)}{2\pi\omega^2 F} \tag{B50}$$

extinction cross section

particle Vol

$$\frac{\sigma_x}{\omega v} = \frac{1}{F\chi_d} = \frac{2\pi\omega^2}{3\sigma P_e^2(1)} \tag{B51}$$

Mass requirement M, for extinction across area A (cm^2)

$$M = A\chi_d\rho = \frac{2\pi\omega^2\rho A}{3\sigma P_{\epsilon(1)}^2} \quad \text{gms} \qquad \text{(B52)}$$

ρ = density of metal (gms / cc)

10. Permittivity of Dielectric Substrate

The permittivity ϵ_B of the material or background sustaining the particle distribution has been, assumed very nearly 1, matched to free space (esu cgs). The explicit form of the composite permittivity ϵ for dilute loadings in terms of ϵ_B, allowing non-unity values, appears as the additional term $\epsilon_B - 1$, added to the permittivity ϵ result for the free space case that assumes $\epsilon_B = 1$, that is,

$$\epsilon(\epsilon_B) = \epsilon_B - 1 + \epsilon(1) \qquad \text{(B53)}$$

When the propagation medium is not free space, all permittivity statements must be interpreted as referring to relative permittivities, relative to the propagation medium.

APPENDIX C

COMMENTS ON PERTURBATION THEORY FOR ITERATION CONVERGENCE

1. Large Depolarizing Factor

When the depolarizing factor, P_e is high, such that $\frac{\sigma}{\omega} P_e >> 1$, $\frac{\sigma}{\omega} P_e$ overwhelmingly dominates in the internal field expression, as in (A29). Since $\frac{\sigma}{\omega}$ is very large, of order 10^7 for Al., the internal field is very closely approximated by $\underline{E} = \frac{i\omega}{\sigma P_e} \underline{E}_o$, with the uncertainty term $\hat{\epsilon}$ bounded as in expressions (A32), (A33) or (A34). The penetration depth δr is bounded by the skin depth δr_{sk} .

$$\delta r \leq \delta r_{sk} = \frac{c}{2\pi} \frac{1}{\sqrt{2\sigma\mu f}} \tag{C1}$$

using δr_{sk} in place of δr_j , δr_r , and the Rayleigh condition

$$k_o R = \frac{2\pi}{\lambda_o} R \leq 1$$

predominance of P_e in the sense of (A31a) is assured when

$$P_e > \sqrt{\frac{\mu f}{2\sigma}} \quad \text{(disk)} \tag{C2}$$

$$\left(\frac{2\pi R}{\lambda_o} < 1\right)$$

$$P_e > \frac{6\pi^2 \hat{\rho}^2}{L \lambda_o} \sqrt{\frac{\mu f}{2\sigma}} \quad \text{(rod)} \tag{C3}$$

2. General Rayleigh Condition for Magnetic Conductors

The lower bounds on P_e are reasonably small enough for non magnetic materials, $\mu \simeq 1$. However when μ is very large, as for ferromagnetic conductors, where $\mu > 10^3$, the restriction on the bounds of P_e is much more limiting.

In order to establish bounds which are independent of μ , the modified Rayleigh condition is more consistent, namely

$$\frac{k_0 R}{\sqrt{\mu}} \lesssim 1 \qquad \text{(modified Rayleigh)} \tag{C4}$$

Then the lower bounds on are independent of

$$P_e(k) > \sqrt{\frac{f}{2\sigma}} \qquad \text{(disk)} \qquad \left(\frac{2\pi R}{\lambda_0 \sqrt{\mu}} \lesssim 1\right) \tag{C5}$$

$$P_e(k) > \frac{6\pi}{L\lambda_0} \rho^{2,1^2} \sqrt{\frac{f}{2\sigma}} \qquad \text{(rod)} \tag{C6}$$

for strong depolarizing effects.

3. Weak Depolarizing Field

Condition (A31(b)) denotes weak depolarization, under which $\underline{E} \approx \underline{E}_0$, i.e. the external field remains uncancelled on the inner surface of the particle. On using bounds (A32), (A33) for penetration distances, certainly bounded less than the thickness of the optimally oriented spheroids, with longer axes parallel to the incident fields, and the limiting values of the depolarizing factors from Table 58A, the ratios of minor to major axes a_1/a_2 for weak depolarization become ...

$$\frac{a_1}{a_2} \leq \frac{1}{1+\frac{\pi}{2}} \frac{f}{\sigma} \qquad \text{(disk)} \qquad \left(\frac{2\pi a_2}{\lambda_0 \sqrt{\mu}} \lesssim 1\right) \tag{C7}$$

$$\frac{a_1}{a_2} \leq \frac{1}{\sqrt{e_{n2}}} \sqrt{\frac{f}{\sigma}} \qquad \text{(rod)} \tag{C8}$$

4. Weak Depolarizing Field Convergence

In the case of (A1b), the internal field integral equation, (A15), can be solved as an iteration sequence, or linear perturbation series about the external field value E_o. Instead of (A15), express the iteration sequence

$$E_k^n = E_{o\,k} - \frac{i\omega\mu\sigma}{c^2}\int d\underline{r}' E_k^{n-1}\psi(R') + \frac{i}{\omega}\sigma\int dS_k\, E_k^{n-1}\partial_{g_k}\psi \tag{C9}$$

where E_k^{n-1} is the n^{th} iterate in approximation and

$$E_k^0 = E_{o\,k} \tag{C10}$$

Now consider the n^{th} difference...

$$\Delta E_k^n \equiv E_k^n - E_k^{n-1} \tag{C11}$$

on substituting in the iteration integral equation, the recursion for ΔE_k^n becomes ...

$$\Delta E_k^n = -\frac{i\,\omega\mu\sigma}{c^2}\int d\underline{r}'\,\Delta E_k^{n-1}\psi(R') + \frac{i}{\omega}\sigma\int dS_k\,\Delta E_k^{n-1}\partial_{g_k}\psi \tag{C12}$$

on taking a norm on ΔE_k^n such as,

$$\|\Delta E_k^n\| = \max_{region} |\Delta E_k(r)| \tag{C13}$$

it follows that

$$\|\Delta E_k^n\| \le \left(\frac{\omega\mu\sigma}{c^2}\hat{\epsilon} + \frac{\sigma}{\omega}P_e\right)\cdot\|\Delta E_k^{n-1}\| \tag{C14}$$

Thus the sequence converges for

$$\frac{\omega\mu\sigma}{c^2}\hat{\epsilon} + \frac{\sigma}{\omega}P_e = \frac{\sigma}{\omega}\left(\frac{\omega^2}{c^2}\mu\hat{\epsilon} + P_e\right) < 1 \tag{C15}$$

or

$$\left(k_o^2\mu\hat{\epsilon} + P_e\right) < \frac{\omega}{\sigma} \tag{C16}$$

Then for a disk or oblate spheroid, for $a_1 << a_2$,

$$k_0^2 \mu \hat{\epsilon} + P_\ell \leq (2\pi + \pi^2) \frac{a_1}{a_2} \qquad \left(\frac{2\pi a_2}{\lambda_0 \sqrt{\mu}} < 1 \right) \tag{C17}$$

Thus if

$$\frac{a_1}{a_2} < \left(\frac{1}{2\pi + \pi^2} \right) \frac{\omega}{2\sigma} = \left(\frac{1}{1 + \frac{\pi}{2}} \right) \frac{f}{\sigma} \tag{C18}$$

it follows that the difference sequence converges to zero faster than

$$\left(\frac{\sigma}{\omega} \left(2\pi \left(1 + \frac{\pi}{2} \right) \frac{a_1}{a_2} \right) \right)^n \tag{C19}$$

and the zeroth approximation

$E_k^0 = E_0$ is bounded in error

$$\| E_k^0 - E_k \| \leq \frac{\alpha_1}{1 - \alpha_1} \quad , \quad \alpha_1 = \frac{\sigma}{\omega} \left(2\pi \left(1 + \frac{\pi}{2} \right) \frac{a_1}{a_2} \right) < 1$$

$$\left(\frac{2\pi a_2}{\lambda_0 \sqrt{\mu}} < 1 \right) \tag{C20}$$

Similarly for a rod or prolate spheroid, the convergence condition is

$$\frac{a_1}{a_2} < \frac{1}{\sqrt{\ell n 2}} \sqrt{\frac{f}{\sigma}} \tag{C21}$$

with a convergence rate faster than $\left(\frac{\sigma}{\omega} \left(\ell n 2 \, \frac{a_1^2}{a_2^2} \right) \right)^n$ and

an error in zeroth approximation bounded as

$$\| E_k^0 - E_k \| \leq \frac{\alpha_2}{1 - \alpha_2} \tag{C22}$$

$$\alpha_2 = \frac{\sigma}{\omega} \left((\ell n 2) \frac{a_1^2}{a_2^2} \right) < 1 \tag{C23}$$

$$\left(\frac{2\pi}{\sqrt{\mu} \lambda_0} < 1 \right)$$

APPENDIX D

EFFECTIVE PERMEABILITY, μ_{eff}, OF A DISTRIBUTION OF FERROMAGNETIC PARTICLES

In analogy with the electrostatic case described in A1, the particle internal magnetic field $\underline{H}_i$ induced by an external field $\underline{H}_e$ is given by the integral equation

$$\underline{H}_i = \underline{H}_e + \frac{\Delta\mu}{\mu_0} \int_S dS_z \, \partial_z \left(\frac{1}{R}\right) \underline{H}_i \qquad \text{(D1)}$$

where Rayleigh particles are assumed, $\frac{k_0 R}{\sqrt{\mu}} \ll 1$

μ_0 is the background permeability

$\Delta\mu = \mu - 1$, particle permeability μ

Then for constant on the mean magnetic polarizability becomes $\bar{\alpha}_n = \dfrac{\Delta\mu}{\left(1 - \frac{\Delta\mu}{\mu_0} P_e\right)}$ (D2)

$P_e = \int dS_z \, \partial_z \left(\frac{1}{R}\right)$ the usual depolarizing factor.

On using the Clausius-Mosotti/Lorenz-Lorentz relations for a distribution of particles ... .

$$\underline{H}_{eff} = \underline{\bar{H}} + \frac{4\pi}{3} \underline{P} \qquad \text{(D3)}$$

$$\underline{B} = \mu_{eff} \underline{\bar{H}} = \underline{\bar{H}} + 4\pi \underline{P} \qquad \text{(D4)}$$

with $\bar{N} \Delta v_p = F$ the volume fraction.

The effective permeability takes the form

$$\mu_{eff} = \frac{1 + \frac{8\pi}{3} \bar{\alpha} F}{1 - \frac{4\pi}{3} \bar{\alpha} F} \qquad \text{(D5)}$$

which for $\frac{\sigma_M}{\mu_0} P_e < 1$, and $M >> 1$

$$\mu_{eff} = \frac{1 + \frac{8\pi}{3} F \Delta M}{1 - \frac{4\pi}{3} F \Delta M} = \frac{1 + \frac{8\pi}{3} F_M}{1 - \frac{4\pi}{3} F_M} \qquad (D6)$$

Thus μ_{eff} can have large values when

$$0 \leq \frac{4\pi}{3} F_M \leq 1$$

APPENDIX E

DEPOLARIZATION SENSITIVITY TO INTERPARTICLE SEPARATION ONE AND TWO DIMENSIONAL MODELS

a) 1 Dimensional Linear array—
consider a line distribution of dipole particles of radius Δ, effective charge $\bar{q}$. This model assumes a constant internal field with the neighboring effects as due to simple dipoles.

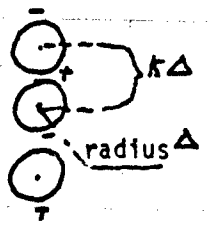

Potential $\phi_1(x,y,z)$

$$\phi_1(x,y,z) = \bar{q} \sum_{N_-}^{N_+} \left(\frac{1}{(x^2+y^2+(z-z_n-\Delta)^2)^{\frac{1}{2}}} - \frac{1}{(x^2+y^2+(z-z_n+\Delta)^2)^{\frac{1}{2}}} \right) \tag{E1}$$

Electric Field at $(0, 0, z_n)$

$$E(0,0,z_n) = -\frac{\partial \phi_1(0,0,z)}{\partial z}\Big|_{z=z_n}$$

$$\approx \frac{2\bar{q}}{\Delta^2} + \bar{q}\frac{\partial^2}{\partial z^2}\left\{ \int_{z_{min}}^{z_{max}} dz' \cdot \frac{1}{(z_n - z')} - \int_{z_{min}}^{z_{max}} dz \frac{1}{(z_n - z)} \right\} \tag{E2}$$

The first term on the right is the internal field in absence of neighbor effects. On performing the differentiation, evaluating at the limits, and setting

$$z_{n+1} = z_n + 2k\Delta \qquad \text{for} \quad k \geq 1 \tag{E3}$$

$$E_z(0,0,z_n) = \frac{2\bar{\rho}}{\Delta^2}\left\{1 - \frac{1}{(2k-1)^2}\right\} \qquad \text{(E4)}$$

It is clear that the internal electrostatic field decreases to zero as

K approaches 1

b) 2 Dimensional distribution.

o o o
o o o
o o o

as in the linear case, the potential

ϕ_2 for the planar distribution is given, on plane x = 0

$$\phi_2(0,y,z) = \bar{\rho} \sum_{N_L}^{N_{y+}} \sum_{N_L}^{N_{z+}} \left(\frac{1}{\left((y-y_m)^2 + (z-z_n-\Delta)^2\right)^{\frac{1}{2}}} - \frac{1}{\left((y-y_m)^2 + (z-z_{n+\Delta})^2\right)^{\frac{1}{2}}} \right)$$

(E5)

The electric field at $(0, y_m^\wedge, z_n^\wedge)$ then is

$$E_z(0, y_m^\wedge, z_n^\wedge) = -\frac{\partial}{\partial z}\Big|_{y_m^\wedge, z_n^\wedge} \phi(0, y, z)$$

$$= \frac{2\bar{\sigma}}{\Delta^2} + \frac{\bar{\sigma}}{\Delta}\frac{\partial^2}{\partial z^2}\left\{ \int_{y_{min}}^{y_{max}} dy' \left\{ \int_{z_{n+1-\Delta}^\wedge}^{z_{max}} dz' \frac{1}{\left((y_m^\wedge - y')^2 + (z_n^\wedge - z')^2\right)^{\frac{1}{2}}} \right.\right.$$

$$\left.\left. - \int_{z_{min}}^{z_{n-1}^\wedge + \Delta} dz' \frac{1}{\left((y_m^\wedge - y')^2 + (z_n^\wedge - z')^2\right)^{\frac{1}{2}}} \right\} \right\} \qquad \text{(E6)}$$

where again the first term on the right is the internal field in absence of neighboring effects. Differentiation with respect to 2, evaluating the limits, integration with respect to y, and again setting

$$z_{n+1}^\wedge = z_n^\wedge + 2k\Delta \qquad k \geq 1 \qquad \text{(E7)}$$

then establishes the field for this simple model as

$$E_z(0, y_m^\wedge, z_n^\wedge) = \frac{2\bar{\sigma}}{\Delta^2}\left(1 - \frac{1}{(2k-1)}\right)$$

2 dimensions.

(E8)

Again, the internal electrostatic field vanishes as K approaches 1, However, the two dimensional array electrostatic field (which in this case is the depolarizing field) is weaker with separation distance, measured as K, than the one dimensional case.

APPENDIX F

ONE AND TWO DIMENSIONAL PROPAGATION MODELS DISPLAYING ZERO DEPOLARIZATION

Here plane wave propagation through distributions of rods and films is modeled. The rod and film scatterers have longitudinal axes parallel to incident $\underline{E}$ vector and normal incidence is assumed on the film planes. It is further assumed that the beam width of the incident field is less than the rod or plate scatterer length. The wave equation in the interior of a "Scatterer" is

$$\left(\underline{\nabla}^2 + \frac{\omega^2}{c^2}\right)\underline{E} = 4\pi i \frac{\omega}{c^2}\sigma \underline{E} \qquad (F1)$$

This is formally transformed into an integral equation through integration of both sides by the free space Green's function.

$$\underline{E} - \frac{i\omega}{c^2}\sigma \int_{\Delta V} d\underline{r} \frac{e^{ik_0|\underline{r}-\underline{r}'|}}{|\underline{r}-\underline{r}'|} \underline{E}(\underline{r}') = \underline{E}_0 \qquad (F2)$$

$\Delta V =$ = vol. of Scatterer

On the assumptions that the effective incident beam width is less than the rod or plate scatterer length, and that the scatterer longitidinal axes or planes are aligned with incident $\underline{E}$ vector, the tangential boundary condition only, applies

$$\underline{\nabla} \times \underline{E} = 0 \implies E_{s+} = E_{s-}$$

The problem is two (rod) or one (plate) dimensional. Thus the depolarizing factor for the geometry is zero, $P_e = 0$.

There are no subsidiary conditions on $\underline{E}(r^1)$, within the volumes ΔV in equation (F 2) and the formal Born perturbation series

$$\underline{E} = \sum_{n=0}^{\infty} \left\{ \frac{i\omega}{c} \sigma \int_{\Delta V} d\underline{r}' \frac{e^{i k_0 |\underline{r}-\underline{r}'|}}{|\underline{r}-\underline{r}'|} \right\}^n \cdot \underline{E}_0 \qquad (r \in \Delta V) \tag{F3}$$

converges to the solution of (F 2) in the interior of the particle if a norm on the integral operator is bounded less than unity

$$\left\| \frac{i\omega}{c} \int d\underline{r} \frac{e^{i k_0 |\underline{r}-\underline{r}'|}}{|\underline{r}-\underline{r}'|} \right\| < 1 \qquad , r \in \Delta V \tag{F4}$$

A sufficient condition for this can be shown to be that the particle (rod, film) thickness Δx be less than skin depth.

$$\Delta x << \sqrt{\frac{c}{\omega} \sigma} \tag{F5}$$

under condition (F 5), the incident field $\underline{E}_0$ closely approximates the internal field $\underline{E}_i$ with an error bound

$$|\underline{E}_i - \underline{E}_0| < \frac{\omega}{c} \sigma \Delta x^2 << 1 \tag{F6}$$

Thus the induced electric dipole moment $\underline{P}$ of the particle is close to

$$\underline{P} \approx \frac{i\omega}{c^2}\sigma\Delta v\,\underline{E}_0 \qquad (F7)$$

with a mean polarization of the distribution as

$$\underline{P} = \frac{i\omega}{c^2}\sigma\bar{F}\,\underline{E} \qquad (F8)$$

where $\bar{F} = \overline{N\Delta v}$ the mean volume fraction.

Because of geometry, the effective field is the mean macroscopic field,

$$E_{eff} = \bar{E} \qquad (F10)$$

Then since effective permittivity ϵ of the distribution is defined as

$$\underline{D} = \epsilon_{eff}\bar{E} = \bar{E} + 4\pi\bar{P} \qquad (F11)$$

It follows that ....

$$\epsilon_{eff} = 1 + i\frac{4\pi}{c^2}\omega\sigma\bar{F} = 1 + i\,4\pi k_0^2\frac{\sigma}{\omega}\bar{F} \qquad (F12)$$

Thus this class of scatterers of thicknesses less then skin depth, is comprised of highly efficient absorbers.

APPENDIX G

VISIT TO NAVAL WEAPONS CENTER

Naval Weapons Center, China Lake Visit

A visit to Dr. Wade Swinford and his colleagues was made on March 20 in order to discuss the Research effort to date and obtain unclassified information concerning recommended emphases of interest.

A review of the work carried out by the undersigned was given.

- starting from the Stratton-Chu form of vector integral equation-
- derivation of approximate internal field with a small spatially varying uncertainity
- application to ellipsoid-spheroid scatterers and the internal field diminishing effect of the depolarizing factor
- the depolarizing factor interpreted as the average interior solid angle subtended by the normally incident electric field
- dipole moment of a particle multiplied by the average particle number density to establish the polarization
- effective particle field in a distribution, giving rise to composite permittivity or dielectric constant via the Lorentz-Lorenz law.
- comparison of low and highly depolarizing particle geometry in determining
  a) dilute concentration absorption - extinction cross section, extinction depth, and mass requirements.
  b) general concentrations to establish power reflection - absorption coefficient and extinction depths as a function of wave length, volume fraction and conductivity: establish condition for total reflection.
- extended analysis of internal field integral equation, including high μ (ferromagnetic) conductors.
  for Rayleigh size particles considered solution to wave equation in spheroidal coordinate which matches the surface, and substitute in the Stratton-Chu based integral equation to evaluate the arbitrary constant. This approach increases the accuracy of the approximation establishing the spatial dependence of the internal field - skin depth attenuation of depolarized field.
- application to metallic shells, coated ultrafine dielectric particles

- summary of extinction lengths, extinction cross sections and mass requirements for resonant and non resonant disks, rods and metal coated spherical nonconducting particles.

Aerosol Expansion

Dr. Swinford has looked at the behavior of aerosol particles in a (near) vacuum, assumed a point source emitting into a segment of a half space and computed the cloud shape hence a composite dielectric medium, in order to estimate the net absorption. The investigation was done numerically using a ray tracing subroutine, hence limiting the sensitivity to the particle properties, distribution and propagation parameters and the peripheral physics. Of interest in this category is the applied problem of determining the distorted, and free space radar cross section of a satellite imbedded in such isotropic media over practically useful frequency bands.

Lower Limit on Particle Size

A more basic topic that Dr. Swinford stressed was of definite interest and remains unanswered is the lower limit of particle size for effectively low depolarization or the maintenance of high absorption to scattering cross section ratio. That is, sizes or dimensions that are less than the conduction electron mean free path, thus having a higher, anomalous collision frequency. The interest is in particle thicknesses of 100 to 1000 atomic diameters.

High Magnetic Permeability

Also indicated as basic and important is the role of high magnetic permeability in the effects mentioned above as well as in potentially modifying the absorptive behavior of particles. Included are the effects of high μ metal coating of fine particles.

APPENDIX H

PAPER PRESENTATION

The paper "Model of Low Frequency Anomalous Propagation Effects in Particulate Contaminated Plasma; was presented orally at the 1981 IEEE International Conference on Plasma Science, May 18, 1981, Santa Fe, New Mexico.(*)

This Appendix contains the Abstract and the Vu-Graphs of the presentation.

(*) Janos, W. A., Paper 12F3, IEEE Conference Record Abstracts, 1981 IEEE International Conference on Plasma Science, May 18-20, 1981, Santa Fe New Mexico.

Abstract submitted for the
1981 IEEE INTERNATIONAL CONFERENCE ON PLASMA SCIENCE
May 18-20, 1981

Model of Low Frequency Anomalous Propagation Effects in Particulate Contaminated Plasma.* WILLIAM A. JANOS, 8381 Snowbird Drive, Huntington Beach, CA, 92646

The presence of metallic particle contaminants in an R.F. probed or driven plasma will modify the medium permittivity. When the particles are of Rayleigh dimensions conditions for strong absorption may be present, depending on particle shape, concentration, conductivity and magnetic permeability.

An overview is presented of the perturbing effects on R.F. induction and propagation due to dilute concentrations of Rayleigh/submicron sized metallic particles. Absorption is primarily emphasized for this low frequency limit case. High reflection effects in resonant cases associated with high particle polarizability are also predicted by the derived composite permittivity but are of more limited validity since they refer to a negative real permittivity limit.

Both coherent and incoherent anomalous propagation effects associated with particulate scattering are considered. A model of the perturbed, frequency dispersive permittivity of a particle-contaminated, two-fluid, charge-neutral plasma is determined using the macroscopic theoretical prescription of Clausius-Mosotti-Lorentz-Lorenz for dilute mixtures. The additional model assumptions are

- uniform distribution of particle sizes
- particle depolarization factors of three generic spheroidal shapes - prolate (rod like), oblate (flake) and sphere.

Conditions for contaminant dominated extinction, phase shift distortion and reflection are discussed in terms of the mean particle properties.

*Work supported by Office of Naval Research Contract N00014-80-C-0926.

STRATTON-CHU GREEN'S THEOREM

INTERNAL FIELD , $\left(\text{SAY } \psi = e^{ik_0 R}/R \right)$

$$\underline{E}_p = \int ds' \left\{ \left(\frac{-i\omega}{c_0^2} \hat{n} \right) \psi \, \underline{J} - \rho \, \underline{\nabla} \psi \right\} + \underline{E}_0$$

$$\underline{J} = \sigma \underline{E}_p \quad , \quad \rho = \rho_s \delta(r - r_s) = \frac{\Delta k}{4\pi k_0} (\hat{e}_i \cdot \hat{n}) E_p$$

$$\frac{\Delta k}{k_0} = \frac{4\pi i \sigma}{\omega} \quad , \text{RAYLEIGH } a < \frac{\lambda}{2\pi}$$

$$\rightarrow \quad E_{is} = \frac{E_{0is}}{1 + \frac{a^2}{4\pi k_0} P_a}$$

DEPOLARIZING FACTOR

$$P_{an} = \int dS_a \frac{\partial}{\partial \beta_a} \left(\frac{1}{R} \right)$$

POLARIZABILITY / VOL. , α_v

$$\alpha_v = \frac{p_i}{\Delta V E_i}$$

DIPOLE MOMENT

$$\underline{p} = \underline{P}\,\Delta V = \underline{J}\,\frac{\Delta V}{i\omega}$$

$$\rightarrow \alpha_v = \frac{-i\sigma}{4\pi\omega}\,\frac{1}{\left(1 + \frac{i\sigma}{4\pi\omega} P_2\right)}$$

POLARIZATION OF DISTRIBUTION

$$\underline{P} = \overline{\alpha_v \Delta V N}\,\underline{E}_{eff}$$

$$\underline{E}_{eff} = \underline{\bar{E}} + \frac{4\pi}{3}\underline{P}$$

$$\rightarrow \quad \epsilon = \epsilon_0 + \frac{\frac{4\pi}{3}\overline{\alpha_v \Delta V N}}{1 - \frac{4\pi}{3}\overline{\alpha_v \Delta V N}} \qquad L\text{-}L,\ \epsilon\text{-}M$$

$$\epsilon_0 \approx 1 - \left(\frac{\omega_p}{\omega}\right)^2 \frac{1}{\left(1 - i\frac{\nu}{\omega}\right)}$$

$$\overline{N_{eq}\alpha V} = \sum_k F_k \alpha_{vk}$$

F_k = VOL. FRACTION OF PARTICLE OF TYPE k

α_{vk} = POLARIZABILITY/VOL.

$$= -i\frac{\sigma}{\omega}\frac{1}{(1+i\frac{\sigma}{\omega}P_e)}$$

CONSIDER 2 CLASSES OF PARTICLES

1) $P_{e1} > \frac{\omega}{\sigma}$, 2) $P_{e2} < \frac{\omega}{\sigma}$

VOLFRACTION F_1 VOL FRACTION F_2

ABSORBING THICKNESS δ_{R_0}

$\delta_{R_0} \leq \delta_{Tsk}$ = SKIN DEPTH.

SOLID PARTICLES, MINIMAL P_e) $a < \lambda/2\pi$

SPHERE $P_e = \frac{\sqrt{\varepsilon}}{3} = \text{CONST.}$

DISK $\sim \left(\frac{a_1}{a_2}\right)$ $a_1 << a_2$

ROD $\left(\frac{a_1}{a_2}\right)^{\sim}$

LORENTZ - LORENZ PERMITTIVITY TENSOR

$$\underline{\underline{\epsilon}} = \underline{\underline{I}} + \underline{\underline{\Delta\epsilon}}_{(\text{PLASMA})}$$

$$+ 4\pi\left(3F_1\left\langle\frac{1}{P_{e_1}}\right\rangle\left\{1 - \frac{i\omega}{\sigma}\left\langle\frac{1}{P_{e_1}}\right\rangle\right\} + \frac{i\sigma}{\delta\omega}F_2\right)\cdot\underline{\underline{I}}$$

(DILUTE CONCENTRATIONS ASSUMED :

$$3F_1\left\langle\frac{1}{P_{e_1}}\right\rangle, \frac{\sigma}{3\omega}F_2 < 1 \quad)$$

WITH e-values FOR PROPAGATION $\perp$ TO $\underline{B}$

$$\epsilon_\pm = 1 - \left(\frac{\omega_p}{\omega}\right)^2\frac{i\omega}{(i\omega+\nu)}\left\{\frac{(i\omega+\nu)^2}{(i\omega+\nu)^2+\omega_B^2} \pm \frac{i(i\omega+\nu)\omega_B}{(i\omega+\nu)^2+\omega_B^2}, 1\right\}$$

$$+ 12\pi F_1\left\langle\frac{1}{P_{e_1}}\right\rangle$$

$$+ i4\pi\left\{\frac{\sigma}{3\omega}F_2 + 3F_1\left\langle\frac{1}{P_{e_1}}\right\rangle^2\right\}$$

INCREMENTS IN

REFRACTIVE INDEX $\Delta Re(n) = 6\pi F_1\left\langle\frac{1}{P_{e_1}}\right\rangle$

ATTENUATION FCTR $\Delta Im(n) = 2\pi\left\{\frac{\sigma}{3\omega}F_2 + 3\left\langle\frac{1}{P_{e_1}}\right\rangle^2 F_1\right\}$

LIMITING CASE

- NEGLIGIBLE DEPOLARIZING DOMINANT, SET $F_1 = 0$
- NEGLIGIBLE PLASMA - ON PERIPHERY OF PLASMA, SET $\omega_i^2 = 0$

$$\epsilon = \frac{1 + 2_i \beta}{1 - i \beta}$$

$$\beta = \frac{4\pi}{9}\frac{\sigma}{\omega} F_2 = \frac{2.10^7}{f(GHz)} F_2 \quad [AL.]$$

NORMAL INCIDENCE :

$$R = \left| \frac{\sqrt{\epsilon} - 1}{\sqrt{\epsilon} + 1} \right|^2$$

$\beta = 40$, $R > 95\% \rightarrow F_2 \geq 2 \times 10^{-5}$ [10 GHz]

$\beta = .07$, $A = 1 - R > 95\% \rightarrow F_2 \geq 3 \times 10^{-8}$ [10 GHz]

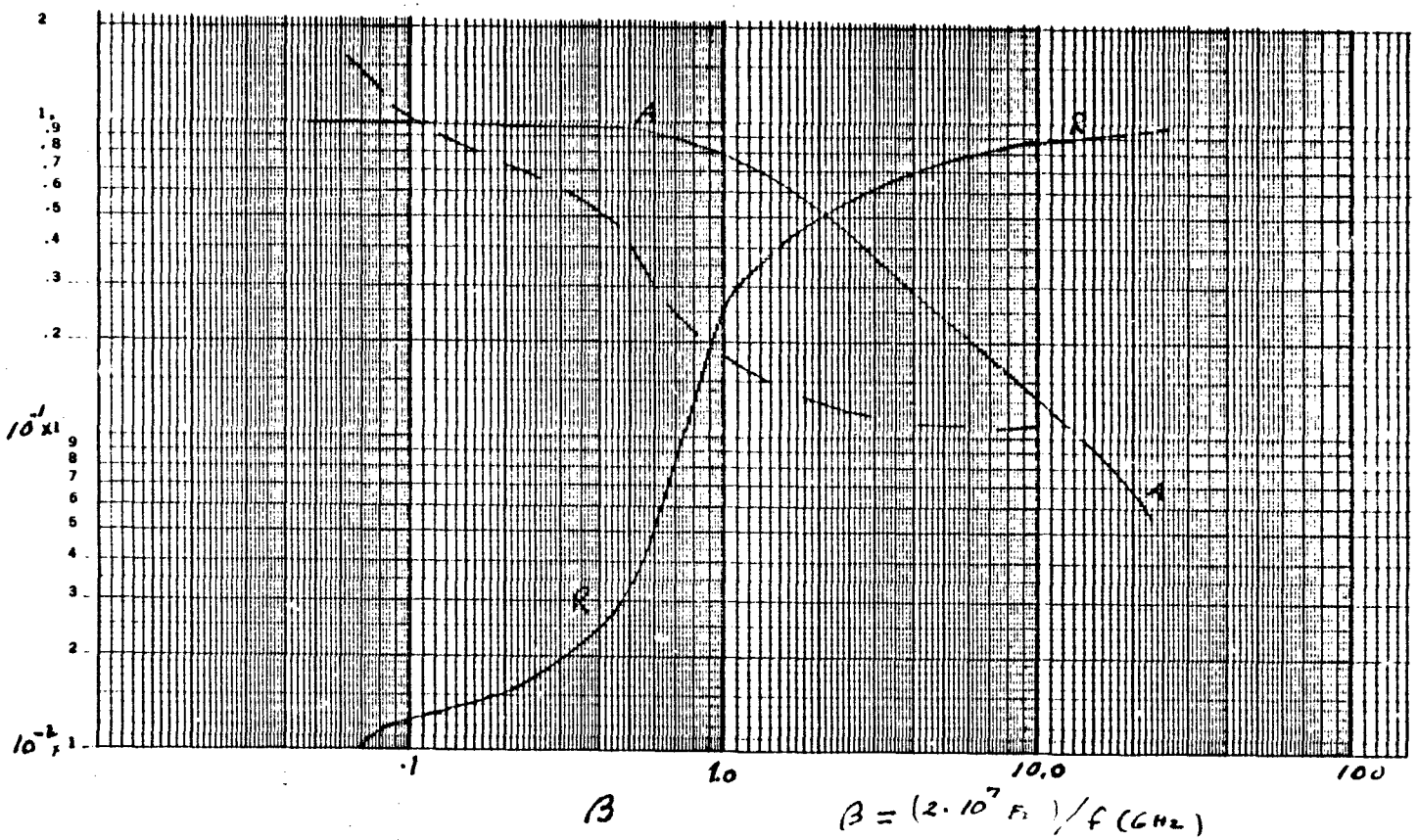

Power Reflection/Absorption of Efficient Absorbers vs β

CERTIFICATION OF NUMBER OF HOURS EXPENDED.

LABOR CATEGORY	NUMBER OF HOURS
(1) Principal Investigator	2080
(1) Secretary - Typist	200

William A. Janos

Dr. William A. Janos

DISTRIBUTION LIST

Scientific Officer
Director, Electronic and Solid State Sciences Program
Physical Sciences Division
Office of Naval Research
800 North Quincy Street
Arlington, Virginia 22217

Attention: Dr. Henry Mullaney

Administrative Contracting Officer
Office of Naval Research Western Regional Office
1030 E. Green Street
Pasadena, California 91106

Attention: Mr. Gordon Chapman

NRLCode 2627
Naval Research Laboratory
Washington, D.C. 20375

ONR Code 102 IP
800 North Quincy Street
Arlington, Virginia, 22217

Defense Documentation Center
Building 5, Cameron Station
Alexandria, Virginia 22314

Naval Weapons Center
Code 3542
China Lake, California 93555

Attention: Dr. Wade Swinford

DISTRIBUTION LIST

Communications Research Laboratory
1411 Stratton Way
Santa Ana, California 92705

Attention: Dr. A.J. Mallinckrodt

UCLA Systems Science Department
Westwood, Los Angeles, California 90024

Attention: Prof. P.K.C. Wang

Spectra Research Systems, Inc.
1811 Quail Street
Newport Beach, California 92660

Attention: M.S. Sandhu

Technology Service Corporation
2950 31st Street
Santa Monica, California 90405

Attention: Dr. Peter Swerling

Aerojet Electro Systems
P.O. Box 296
Azusa, California 91702

Attention: J.W. Wheeler 170/SL21
M. Loring 170/SL72

Advanced Kinetics, Inc.
1291 Victoria Street
Costa Mesa, California 92627

Attention: Dr. Ralph W. Waniek

Emerson & Cuming, Inc.
Canton, Massachusetts 02021

Attention: F.J. Luoma